The Reliable Hub-and-spoke Design Problem: Models and Algorithms

Yu An, Yu Zhang and Bo Zeng

May, 2011

Abstract

This paper presents a study on reliable single and multiple allocation hub-and-spoke network design problems where disruptions at hubs and the resulting hub unavailability can be mitigated by backup hubs and alternative routes. It builds nonlinear mixed integer programming models and presents linearized formulas. To solve those difficult problems, Lagrangian relaxation and Branch-and-Bound methods are developed to efficiently obtain optimal solutions. Numerical studies of proposed solution methods on practical instances are reported, along with a few insights of system design.

Key words: reliable network design; hub-and-spoke; Lagrangian Relaxation; Branch-and-Bound

1 Background and Motivation

The hub-and-spoke system has been widely employed in various industrial applications. It is a fully connected network with material/information flow between any two nodes being processed at a small number of critical nodes (i.e. *hubs*) and moved through inter-hub links. Compared with the one built with the point-to-point structure, it has a much smaller number of links. Also, because traffic flows are consolidated by hubs and inter-hub links, significantly less operating cost can be achieved because of economies of scale. Given such advantages, industry companies including airlines, logistics companies, and telecommunications firms extensively utilize the hub-and-spoke architecture to reduce the construction and operating costs.

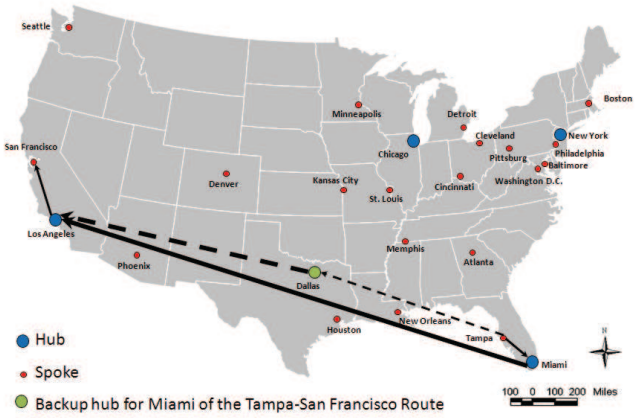

Figure 1: Regular and Alternative Routes

Traditionally, the primary concern of hub-and-spoke network design is the locations of hub facilities and the allocations of non-hub nodes (i.e. *spokes*) to hubs such that the cost of transportation and construction is minimized. The first quantitative model was introduced by [30, 31, 32] on a data set describing airline passenger flows between any pair of 25 US major cities in 1970s, which is often referred to as Civil Aeronautics Board (CAB) data set. In practical operations, the most vexing issue of a hub-and-spoke system is its vulnerability. Given the fact that flows are consolidated and processed at hubs, disruptions, degradations or even congestions at hubs could significantly deteriorate the performance of the hub-and-spoke system. Such an issue is most prominently demonstrated in air transportation where natural disasters, severe weather, labor strikes or terrorism threats will disrupt the regular operations and make airports partially or completely unavailable. A recent example is that Iceland volcano eruption in 2010 disabled two international hubs, i.e. Heathrow in UK and de Gaulle in France, and resulted in numerous trans-Atlantic flight cancelations. Furthermore, single disruption events often resonate network-wide, drastically degrading the performance of the entire airline network with enormous economic losses. For example, over 10 million passengers worldwide were stranded by volcano ashes, see [1].

To deal with the vulnerability issue, several mitigation strategies have been proposed and implemented. Those strategies include delaying, canceling and rerouting in air transportation [23, 3] and network peering in telecommunications systems [34]. However, most of them are re-active strategies which are often costly, difficult to implement and inefficient

due to the initial system design. To address this issue, we propose to explicitly include the hub unavailability in the hub-and-spoke network design to build reliable systems. Especially, alternative route decisions in the case of disruptions will be included. As illustrated in Figure 1, the solid line denotes the regular route for the flow from Tampa to San Francisco and the dot line denotes an alternative route if Miami hub is not available. With this strategy, we construct a new type of optimization models for hub-and-spoke design problem, which minimizes the operating cost from both normal and disruptive situations. However, the introduction of backup hubs and alternative routes drastically increases the complexity of those models, compared to classical hub-and-spoke design models. To solve the resulting large-scale (nonlinear) mixed integer programs, we investigate their structures and develop various solution methods.

To the best of our knowledge, our study is the first analytical work on the reliable hub-and-spoke design with consideration of backup hubs and alternative routes. Also, different from most of algorithms designed for reliable facility location problems, the developed Lagrangian relaxation algorithm does not require special properties and is easy to implement. Our computational study on practical instances shows that the resulting hub-and-spoke designs are robust to hub unavailability. As a result, our study yields a set of useful tools for practitioners, such as airlines, to re-structure their networks or to identify strategic partners to hedge against various disruptions and achieve better performance. For example, the recent merger between United and Continental Airlines brings the new United Airlines eight domestic hubs, which probably are more than enough. So, our models and algorithms can be applied to identify those for closure, if the number of hubs will be reduced and hub unavailability is considered.

The paper is organized as follows. In Section 2, we present a brief literature review on hub-and-spoke design and recent research on reliable facility location models. In Section 3, we study the reliable single allocation hub-and-spoke model and describe our solution methods. In Section 4, we extend our study to the reliable multiple allocation hub-and-spoke model. In Section 5, we report computational results of developed solution methods on CAB data set and present a few insights on system design. Section 6 concludes this paper with some discussions on future research directions.

2 Literature Review

Hub-and-spoke design problem is conventionally called *hub location problem* (HLP), which is concerned with locating hub facilities and allocating demand nodes to hubs. There are generally two basic structures: single allocation (SA) and multiple allocation (MA). In SA hub-and-spoke model, all inbound/outbound flows of any node must be routed through a specific hub before proceeding to their destination(s). In MA model, flows from a given source node go through different hubs depending on their destinations, see Figure 2 for the differences between them. In the remainder of this paper, we use SA-HLP or MA-HLP to denote the corresponding design problem. When the number of hubs (p) is given, the problem is called the p-hub median problem, or p-hub problem for short. [32] proposes the first mathematical formulation for p-hub HLP and presents the first quantitative analysis on this network structure using CAB data set. Since then, as hub-and-spoke structures are of significant theoretical and practical values, a large number of papers have been published on developing models with practical features and on designing efficient algorithms.

We first briefly describe a few important results on formulation and algorithm design. Ernst and Krishnamoorthy [15] and Ernst and Krishnamoorthy [16] formulate SA and MA p-hub HLP, respectively, based on the idea of "multicommodity flow". [37] propose mixed integer formulations for both SA and MA p-hub HLPs that yield tight linear relaxations. As for the customized algorithm development, Ernst and Krishnamoorthy [17] develop shortest-path based Branch-and-Bound algorithms for the formulations in [15] and [16]. In solving the MA p-hub HLP, the Branch-and-Bound process starts with a cluster of root nodes instead of a single node to improve the initial lower bound. As a result, it is able to obtain exact solutions for problems with up to 200 nodes within acceptable amount of time. A similar strategy is also applied to SA p-hub HLP. Pirkul and Schilling [35] propose a Lagrangian relaxation approach to the SA p-hub model presented in Skorin-Kapov et al. [37]. By adding a new type of cut constraints, their algorithm is very effective in generating optimal solutions. Different from the p-hub problem, the *hub location problem with fixed cost* seeks to minimize the transportation cost and the construction cost where a fixed construction cost is associated with a decision of hub location. O'Kelly [33] and Campell [4] study a few formulas of fixed cost HLP. There also exist many literatures in search of effective solution algorithms for these problems, see [10], [7] and [5] for examples. We mention that [20] explore the polyhedral aspect of HLP and [21] develop a method of lifting

facets from facility location problems(FLPs) to HLPs and derive a tighter formulation for MA fixed cost HLP. One may refer to [2] for a comprehensive review of modeling techniques and solution methods of HLP. In the remainder of this paper, unless we explicitly mention, the hub-and-spoke network design problem indicates p-hub problem.

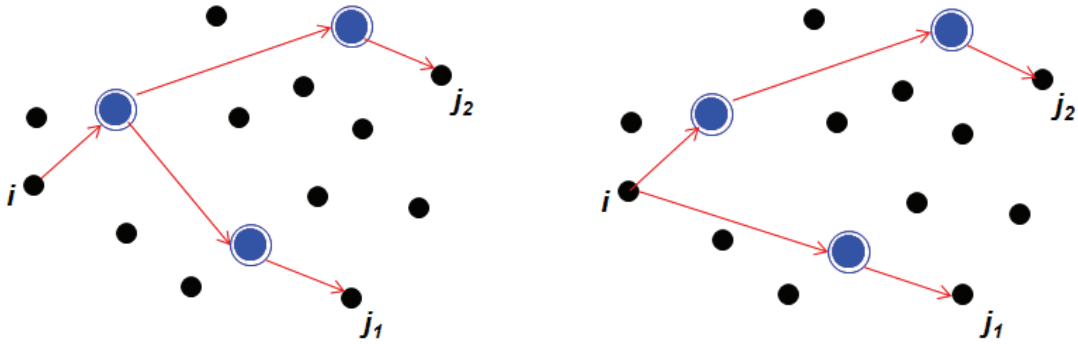

(a) SA Hub-and-spoke Structure (b) MA Hub-and-spoke Structure

Figure 2: Single Assignment and Multiple Allocation Hub-and-spoke Structures

Recent study focuses on extending classical SA and MA models by incorporating advanced practical features, such as the congestion effect and the nonlinear economies of scale, and developing more sophisticated solution algorithms. Minimizing the transportation cost tends to force the traffic flows to go through a small number of hubs, which leads to the congestion issue at hubs. The work in [19] is among the first to study the effects of congestion on hub-and-spoke networks. In general, congestion effects are tackled with by either adding capacity constraints or adding a congestion cost term to the objective function. [13] is probably the first one to model the exponential nature of congestion effects by explicitly adding the congestion cost to the objective function of a SA model. Following this thread, [11] further study the congestion effects of MA fixed cost HLP and use generalized Benders Decomposition to cope with the exponential congestion cost. Since the congestion effects will reduce the benefit of hub-and-spoke network, the authors also suggest to allow direct service between nodes and expanding capacities of hubs. [14] extend SA-HLP by considering the congestion cost and capacity selection at the same time, where the congestion cost is a function of flow and capacity. A customized cutting plane method is used to deal with the nonlinearity. One can refer to [11] for a brief review on the study of congestion. Although it is generally assumed in most literatures that all inter-hub transportation takes

the same discount factor, this assumption oversimplifies the impact of economies of scale on network design. [12] consider this issue by introducing a flow-dependent economies of scale to MA fixed cost HLP and develop a Benders Decomposition procedure to solve the resulting model. Recently, [8] propose a multi-period MA fixed cost HLP to study the dynamic network structure in real applications where costs and demands vary over the planning horizon and the hub location and spoke allocation decisions can be made for each time period. For the resulting large-scale integer program, they combine Lagrangian relaxation, variable fixing techniques, and a Branch-and-Bound scheme to obtain optimal solutions.

Nearly all studies on HLP assume that the chosen hubs will always operate as planned. Nevertheless, as the typical cases in air transportation industry, adverse weather often significantly deteriorates the availability of a hub airport and results in huge failure costs. Similar situations have been seen in supply chain or logistics networks where facilities play the central role in providing services to customers. To deal with facility disruptions, a facility location model with backup strategy, referred to as the *reliable facility location model*, was introduced by [38] and received significant attention. [38] seek to minimize the expected transportation cost (and construction cost if fixed cost from construction is included) generated by receiving service from normal and backup facilities under an assumption that all nodes have the same unavailability. [9] relax the assumption of equal facility unavailability. [26] extend this direction by considering correlated unavailability among facilities. Lim et al. [28] extend the research by considering two types of facilities, one is completely available and the other is unreliable. Li et al. [25] consider the reliable model with a fortification budget and fortification decisions. Nevertheless, those reliable facility location models are difficult discrete optimization problems and state-of-the-art commercial solvers often fail to generate good solutions in a reasonable time for practical instances. To derive optimal solutions, Lagrangian relaxation based algorithms, and their Branch-and-Bound extensions, are the major solution strategies, see [38, 26, 9, 28, 25]. However, when unavailability is node-specific, reliable facility location models will have many nonlinear terms, whose linearizations will introduce enormous number of variables and constraints [9, 25] and make Lagrangian relaxation algorithms less efficient. Under this situation, approximation algorithms [26, 9] have been developed to efficiently obtain good solutions.

Although the research on reliable facility location models has attracted many researchers, up to now, only two recent papers consider reliable hub-and-spoke networks. In [24], given

that each arc or hub has a reliability (same as availability in this paper), they build SA and MA models to derive an optimal network structure that maximizes the expected network flow, without considering backup hubs and alternative routes. In [39], reliable SA and MA models with consideration of hub unavailability and alternative routes have been developed and a heuristic algorithm has been implemented. The authors observe that, different from the reliable facility location model, reliable hub-and-spoke models are much more complicated. First, as each route has two connecting hubs, two backup hubs may be needed to maintain an connectivity with economic advantages in the case of disruptions. This requirement drastically increases the size of the model. Second, overall transportation cost is determined by interactive hubs. Their interactions have a more significant impact on network design if backup hubs and alternative routes are included. Third, even hubs are fixed, spoke allocations, especially in single allocation structure, cannot be simply determined by spoke-hub distances. Due to those challenges, to the best of our knowledge, little analytical research has been done on analyzing and solving reliable hub-and-spoke models with backup hub and alternative route decisions. Nevertheless, hub-and-spoke models play a critical role in many transportation and telecommunications industries where system reliability is of extremely high importance. So, we propose to systematically study the reliable hub-and-spoke models and develop efficient algorithms to solve practical instances and advance the research in designing reliable network systems.

3 The Reliable Single Allocation Hub-and-spoke Model

As we mentioned earlier, hub disruptions and the resulting hub unavailability can be mitigated by allowing part or all disrupted flows to take alternative routes through backup hubs. To avoid congestions resulted from alternative routing, we adopt the MA structure in designing alternative routes, regardless of the SA or MA structure in regular routes. In this section, we present our study on the reliable SA model, denoted by *R-SAHLP*, in details and describe a related work on the reliable MA model, denoted by *R-MAHLP*, in Section 4. Throughout this paper, we denote a flow by its source and destination nodes, i.e. an $i-j$ flow where i is the source and j is the destination. Because the failure probability, i.e. the unavailability, of each hub is typically small, we assume that no more than one hub will be disrupted at any time, which could also be treated as an approximation to the real situation. To minimize the deviation to the regular route, we require that an alternative

route of a flow is just one hub different from its regular route. This rule is realistic and is also compatible with the aforementioned assumption. One implication is that two-hub route needs two alternative routes (which could be identical) to handle hub disruptions and a single-hub route just needs a single-hub alternative route.

In remainder of this section, we first give the (nonlinear) mathematical formulation of *R-SAHLP* and analyze its computation complexity. Then, we present two formulas obtained by different linearization techniques. Finally, we describe a Lagrangian relaxation (LR) algorithm and a Branch-and-Bound framework that can efficiently produce optimal solutions.

3.1 Reliable SA Model: Definition and Formulation

In single allocation problem, every node is assigned to a single hub and all the inbound and outbound flows of this node are routed through that hub. Let $\mathbf{N}$ be the set of nodes and $\mathbf{H} \subseteq \mathbf{N}$ be the set of candidate hub locations. Without loss of generality, we simply assume that $\mathbf{H} = \mathbf{N}$ throughout this paper. Each route can be represented by a 4-tuple, (i, k, m, j) where i and j represent the source and destination respectively and k and m represent the first and the second hub on the route. Each hub m has its own unavailability (i.e. failure probability) q_m. To capture the situation where there is just a single hub on a route (i, k, m, j), i.e. $k = m$, we define q_m^k such that q_m^k equals 0 if $k = m$ and q_m otherwise. Unit transportation cost between a pair of nodes i and j is c_{ij} and the traffic volume between them is w_{ij}. A discount factor from economies of scale, $0 < \gamma < 1$, will be applied to the inter-hub links. So, for $i - j$ flow taking the route (i, k, m, j), the cost of transporting one unit flow is derived as $F_{ikmj} = c_{ik} + \gamma c_{km} + c_{mj}$.

Variables used in *R-SAHLP* include the hub location and allocation variable $\mathbf{Y}$, the

route variable $\mathbf{X}$ and the backup hub variables $\mathbf{U}$ and $\mathbf{V}$.

$$Y_{ik} = \begin{cases} 1, & \text{if node } i \text{ is assigned to hub } k, \\ 0, & \text{otherwise;} \end{cases}$$

$$X_{ikmj} = \begin{cases} 1, & i-j \text{ flow is routed through hubs } k \text{ and } m, \\ 0, & \text{otherwise;} \end{cases}$$

$$U_{ijn} = \begin{cases} 1, & \text{hub } n \text{ is the backup hub for the first hub in the route of } i-j \text{ flow}, \\ 0, & \text{otherwise;} \end{cases}$$

$$V_{ijn} = \begin{cases} 1, & \text{hub } n \text{ is the backup hub for the second hub in the route of } i-j \text{ flow}, \\ 0, & \text{otherwise.} \end{cases}$$

Most literatures assume that traffic and distance between any two nodes are symmetric. We take this assumption in our formulation to reduce the problem size. Note that this assumption indicates that the first backup hub for route (i,k,m,j) will be the second one for route (j,m,k,i). So, we can just consider flows with $j > i$ in our study. Next, we present *R-SAHLP* that generalizes and extends the classical SA hub-and-spoke model developed by [37]. To keep our model trackable and to focus on the impacts of hubs' unavailabilities, our reliable models do not consider the loss of traffic due to spoke disruptions.

$\underline{R-SAHLP}$

$$\begin{aligned} \min \ & \sum_i \sum_k \sum_m \sum_{j>i} F_{ikmj} w_{ij} (1 - q_k - q_m^k) X_{ikmj} \\ & + \sum_i \sum_{k \neq i} \sum_{m \neq k} \sum_{j>i} \sum_n F_{inmj} w_{ij} q_k X_{ikmj} U_{ijn} \\ & + \sum_i \sum_{k \neq m} \sum_{m \neq j} \sum_{j>i} \sum_n F_{iknj} w_{ij} q_m X_{ikmj} V_{ijn} \\ & + \sum_i \sum_{k \neq i,j} \sum_{j>i} \sum_n F_{innj} w_{ij} q_k X_{ikkj} U_{ijn} + \sum_i \sum_{j>i} \phi_{ij} w_{ij} (q_i Y_{ii} + q_j Y_{jj}) \end{aligned} \tag{1}$$

subject to

$$\sum_m X_{ikmj} = Y_{ik} \qquad \forall i, j > i, k \tag{2}$$

$$\sum_k X_{ikmj} = Y_{jm} \qquad \forall i, j > i, m \tag{3}$$

$$\sum_k Y_{ik} = 1 \qquad \forall i \tag{4}$$

$$\sum_k Y_{kk} = p \tag{5}$$

$$U_{ijk} + \sum_m X_{ikmj} \leq Y_{kk} \qquad \forall i, j > i, k \tag{6}$$

$$\sum_k U_{ijk} = 1 - \sum_m X_{iimj} - \sum_m X_{ijmj} \qquad \forall i, j > i \tag{7}$$

$$V_{ijm} + \sum_k X_{ikmj} \leq Y_{mm} \qquad \forall i, j > i, m \tag{8}$$

$$\sum_m V_{ijm} = 1 - \sum_k X_{ikjj} - \sum_k X_{ikij} \qquad \forall i, j > i \tag{9}$$

$$X_{ikmj} \in \{0,1\}\ \forall i, j > i, k, m;\ Y_{ik} \in \{0,1\}\ \forall i, k;\ U_{ijk}, V_{ijk} \in \{0,1\}\ \forall i, j > i, k \tag{10}$$

In the *R-SAHLP*, the objective function is the expected transportation cost considering both the regular situation and the disruptive situation. Specifically, the first term is the regular transportation cost weighted by the probability that both hubs operate normally in the route of each $i-j$ flow. Since we assume that at most one hub will be disrupted, this probability is computed as $1-q_k-q_m^k$. Note from the definition of q_m^k that the probability equals to $1-q_k-q_m$ if two hubs are different and reduces to $1-q_k$ when hubs k and m are identical. The second term represents the transportation cost of routing the flow through the alternative hub when the first hub is disrupted. This is only true for the case where the source of the flow is not a hub because if the source and the first hub are identical, i.e. $i=k$, when the hub fails, there will be no outbound traffic from the hub (source) node. Similarly, the third term represents the cost if the second hub is disrupted and the fourth term represents such cost when there is only one hub on the route and it is disrupted. The last term in the objective function is introduced to penalize the loss of flows in disrupted situations if the source or destination is a hub. Because our model is to minimize the expected transportation cost, which tends to select less reliable nodes as hubs, the penalty from the last term will help to remove such impact. In our numerical study, ϕ_{ij} is set to $2c_{ij}$ for $j > i$.

Constraints (2)-(5) are classical constraints for SA p-hub problem [37]. Constraints (6)

and (8) ensure that the regular hubs and the backup hubs of any flow can only be the nodes chosen to be hubs and the regular hubs and the backup hubs must be different. Constraints (7) and (9) are used to eliminate the cases where either the source or the destination node of a flow is a hub. Because the disrupted hub cannot generate outbound traffic or receive inbound traffic, there is no need to design alternative routes for this flow.

Next, we give the complexity of *R-SAHLP* based on the existing study on the SA hub-and-spoke model.

Proposition 1. (*i*) *The R-SAHLP problem is an NP-hard problem;* (*ii*) *if all hubs are fixed, the route decision problem is an NP-hard problem;* (*iii*) *if all hubs and spoke allocations are fixed, the problem of regular and alternative route design is polynomial solvable.*

Proof. Statements in (*i*) and (*ii*) follow from the fact that when nodes are fully reliable *R-SAHLP* reduces to traditional SA hub-and-spoke model, which has been proven to be NP-hard even hubs are fixed [2]. When hubs and all spoke allocations are fixed, (*iii*) simply follows from two facts that: first, optimal regular routes are completely determined by SA structure; second, optimal backup hubs and alternative routes can be determined by enumerating hubs in the network. □

R-SAHLP is an integer quadratic program as its objective function has multiple terms that involve products of two binary variables. Clearly, using linearization techniques that introduces extra variables and constraints, *R-SAHLP* can be converted into a mixed integer program and supplied to any off-the-shelf mixed integer programming solver to compute optimal solutions. In Section 3.2, we present results from two different linear reformulation approaches that have very different problem sizes. However, we observe that solvers are not efficient to solve practical instances. So, it motivates us to develop an efficient Lagrangian relaxation algorithm, in Section 3.3, without applying linearization techniques to take advantage of the network structure.

3.2 Linear Models from Linear Reformulation

In this section, we first give a linear reformulation for *R-SAHLP* obtained by using standard linearization techniques [29], which is denoted by *StdLinear*. Then, we present a novel linear reformulation for *R-SAHLP* that only introduces a small number of variables and constraints. As it is much more compact than *StdLinear*, we denote it by *CptLinear*.

StdLinear

$$\begin{aligned}\min\ & \sum_i \sum_k \sum_m \sum_{j>i} F_{ikmj} w_{ij} (1 - q_k - q_m^k) X_{ikmj} \\ & + \sum_i \sum_{k\neq i} \sum_{m\neq k} \sum_{j>i} \sum_n F_{inmj} w_{ij} q_k Z_{ikmjn,1} \\ & + \sum_i \sum_{k\neq m} \sum_{m\neq j} \sum_{j>i} \sum_n F_{iknj} w_{ij} q_m Z_{ikmjn,2} \\ & + \sum_i \sum_{k\neq i,j} \sum_{j>i} \sum_n F_{innj} w_{ij} q_k Z_{ikkj,1} + \sum_i \sum_{j>i} \phi_{ij} w_{ij} (q_i Y_{ii} + q_j Y_{jj})\end{aligned}$$

subject to

$$(2) - (10)$$

$$Z_{ikmjn,1} \leq X_{ikmj},\ Z_{ikmjn,1} \leq U_{ijn},\ Z_{ikmjn,1} \geq X_{ikmj} + U_{ijn} - 1 \quad \forall i,k,m,j > i,n$$

$$Z_{ikmjn,2} \leq X_{ikmj},\ Z_{ikmjn,2} \leq V_{ijn},\ Z_{ikmjn,2} \geq X_{ikmj} + V_{ijn} - 1 \quad \forall i,k,m,j > i,n$$

$$Z_{ikmjn,1}, Z_{ikmjn,2} \geq 0 \quad \forall\ i,k,m,j > i,n$$

Compared with the quadratic form in (1)-(10), $X_{ikmj}U_{ijn}$ is replaced by $Z_{ikmjn,1}$ and $X_{ikmj}V_{ijn}$ is replaced by $Z_{ikmjn,2}$. Also, a few sets of constraints are added to enforce that $Z_{ikmjn,1} = X_{ikmj}U_{ijn}$ and $Z_{ikmjn,2} = X_{ikmj}V_{ijn}$.

In fact, compared to the quadratic formula, this mixed integer linear reformulation has to deal with a huge number, $O(|\mathbf{N}|^5)$, of extra variables and constraints. For example, for a small size problem with 10 nodes, linearization leads to roughly 100,000 new variables and $300,000$ new constraints, which is very difficult for professional solvers to generate solutions in a reasonable time. To address this issue, we adopt a recent linearization strategy [6, 36, 22] and create the following compact reformulation *CptLinear*. We mention that this linear formula distinguishes itself by the fact that the number of variables does little change and the number of constraints just linearly increases.

CptLinear

$$\begin{aligned}\min\ & \sum_i \sum_k \sum_m \sum_{j>i} F_{ikmj} w_{ij} (1 - q_k - q_m^k) X_{ikmj} \\ & + \sum_i \sum_{j>i} \sum_n (\Omega_{ijn} - \sigma_{ij} U_{ijn}) \\ & + \sum_i \sum_{j>i} \sum_n (\Theta_{ijn} - \sigma_{ij} V_{ijn}) \\ & + \sum_i \sum_{j>i} \sum_n (\Gamma_{ijn} - \sigma_{ij} U_{ijn}) + \sum_i \sum_{j>i} \phi_{ij} w_{ij} (q_i Y_{ii} + q_j Y_{jj})\end{aligned}$$

subject to

$$(2) - (10)$$

$$\sum_{k\neq i}\sum_{m\neq k} w_{ij}q_k F_{inmj} X_{ikmj} - s_{ijn} + \sigma_{ij} = \Omega_{ijn} \qquad \forall i, j > i, n \tag{11}$$

$$s_{ijn} \leq (\mu_{ij} + \sigma_{ij})(1 - U_{ijn}) \qquad \forall i, j > i, n \tag{12}$$

$$\sum_{k\neq m}\sum_{m\neq j} w_{ij}q_m F_{iknj} X_{ikmj} - t_{ijn} + \sigma_{ij} = \Theta_{ijn} \qquad \forall i, j > i, n \tag{13}$$

$$t_{ijn} \leq (\mu_{ij} + \sigma_{ij})(1 - V_{ijn}) \qquad \forall i, j > i, n \tag{14}$$

$$\sum_{k\neq i, k\neq j} w_{ij}q_k F_{innj} X_{ikkj} - r_{ijn} + \sigma_{ij} = \Gamma_{ijn} \qquad \forall i, j > i, n \tag{15}$$

$$r_{ijn} \leq (\mu_{ij} + \sigma_{ij})(1 - U_{ijn}) \qquad \forall i, j > i, n \tag{16}$$

$$\Omega_{ijn}, s_{ijn}, \Theta_{ijn}, t_{ijn}, \Gamma_{ijn}, r_{ijn} \geq 0 \qquad \forall i, j > i, n \tag{17}$$

where $\mu_{ij} = w_{ij} \max\limits_{k,m}\{F_{ikmj}\} \max\limits_{k}\{q_k\}$, and $\sigma_{ij} \geq 0$ is a predetermined coefficient for $i, j > i$. The linearizataion for the quadratic term $\sum\limits_{i}\sum\limits_{k\neq i}\sum\limits_{m\neq k}\sum\limits_{j>i}\sum\limits_{n} F_{inmj} w_{ij} q_k X_{ikmj} U_{ijn}$ in *R-SAHLP* is completed by new variables Ω_{ijn}, s_{ijn} and constraints (11) and (12). Similarly, Θ_{ijn}, t_{ijn}, (13) and (14) are used for linearization of $\sum\limits_{i}\sum\limits_{k\neq m}\sum\limits_{m\neq j}\sum\limits_{j>i}\sum\limits_{n} F_{iknj} w_{ij} q_m X_{ikmj} V_{ijn}$; Γ_{ijn}, r_{ijn}, (15) and (16) are for $\sum\limits_{i}\sum\limits_{k\neq i,j}\sum\limits_{j>i}\sum\limits_{n} F_{innj} w_{ij} q_k X_{ikkj} U_{ijn}$. Clearly, the number of variables introduced is $O(|\mathbf{N}|^3)$ and the number of the constraints introduced is $O(|\mathbf{N}|^3)$. Given that the quadratic formula has $O(|\mathbf{N}|^4)$ variables and $O(|\mathbf{N}|^3)$ constraints, *CptLinear* formula does not increase the model's complexity. Next, we show that solving *CptLinear* leads to an optimal solution to quadratic *R-SAHLP*.

Let $\Phi(\mathbf{X}, \mathbf{Y}, \mathbf{U}, \mathbf{V})$ to denote the objective function value of *R-SAHLP* for a solution $(\mathbf{X}, \mathbf{Y}, \mathbf{U}, \mathbf{V})$ and $\Psi(\mathbf{X}, \mathbf{Y}, \mathbf{U}, \mathbf{V}, \mathbf{\Omega}, \mathbf{s}, \mathbf{\Theta}, \mathbf{t}, \mathbf{\Gamma}, \mathbf{r})$ to denote the objective function value of *CptLinear* for a solution $(\mathbf{X}, \mathbf{Y}, \mathbf{U}, \mathbf{V}, \mathbf{\Omega}, \mathbf{s}, \mathbf{\Theta}, \mathbf{t}, \mathbf{\Gamma}, \mathbf{r})$.

Proposition 2. *If $(\mathbf{X}^*, \mathbf{Y}^*, \mathbf{U}^*, \mathbf{V}^*, \mathbf{\Omega}^*, \mathbf{s}^*, \mathbf{\Theta}^*, \mathbf{t}^*, \mathbf{\Gamma}^*, \mathbf{r}^*)$ is an optimal solution to Cpt-Linear, then $(\mathbf{X}^*, \mathbf{Y}^*, \mathbf{U}^*, \mathbf{V}^*)$ is an optimal solution to R-SAHLP. Further, we have*

$$\Psi(\mathbf{X}^*, \mathbf{Y}^*, \mathbf{U}^*, \mathbf{V}^*, \mathbf{\Omega}^*, \mathbf{s}^*, \mathbf{\Theta}^*, \mathbf{t}^*, \mathbf{\Gamma}^*, \mathbf{r}^*) = \Phi(\mathbf{X}^*, \mathbf{Y}^*, \mathbf{U}^*, \mathbf{V}^*).$$

Proof. We first show that $(\mathbf{X}^*, \mathbf{Y}^*, \mathbf{U}^*, \mathbf{V}^*)$ is a feasible solution to *R-SAHLP* and

$$\Psi(\mathbf{X}^*, \mathbf{Y}^*, \mathbf{U}^*, \mathbf{V}^*, \mathbf{\Omega}^*, \mathbf{s}^*, \mathbf{\Theta}^*, \mathbf{t}^*, \mathbf{\Gamma}^*, \mathbf{r}^*) = \Phi(\mathbf{X}^*, \mathbf{Y}^*, \mathbf{U}^*, \mathbf{V}^*).$$

Then, we prove that $(\mathbf{X}^*, \mathbf{Y}^*, \mathbf{U}^*, \mathbf{V}^*)$ is an optimal solution to *R-SAHLP*.

It is clear that $(\mathbf{X}^*, \mathbf{Y}^*, \mathbf{U}^*, \mathbf{V}^*)$ is feasible to *R-SAHLP* as it satisfies all the constraints (2) - (10). By multiplying U^*_{ijn} to both sides of (11) and sum them up over all $i, j > i, n$, we obtain $\sum_i \sum_{k\neq i} \sum_{m\neq k} \sum_{j>i} \sum_n F_{inmj} w_{ij} q_k X^*_{ikmj} U^*_{ijn} - \sum_i \sum_{j>i} \sum_n s^*_{ijn} U^*_{ijn} + \sum_i \sum_{j>i} \sum_n \sigma_{ij} U^*_{ijn} = \sum_i \sum_{j>i} \sum_n \Omega^*_{ijn} U^*_{ijn}$. Because of (12), the nonnegativity of s_{ijn} and the fact that U_{ijn} is a binary variable, we have $s^*_{ijn} U^*_{ijn} = 0, \forall i, j > i, n$. Then, to show $\sum_i \sum_{j>i} \sum_n (\Omega^*_{ijn} - \sigma_{ij} U^*_{ijn}) = \sum_i \sum_{k\neq i} \sum_{m\neq k} \sum_{j>i} \sum_n F_{inmj} w_{ij} q_k X^*_{ikmj} U^*_{ijn}$, it suffices to show $\sum_i \sum_{j>i} \sum_n \Omega^*_{ijn} U^*_{ijn} = \sum_i \sum_{j>i} \sum_n \Omega^*_{ijn}$, which reduces to prove that $\Omega^*_{ijn} = 0$ when $U^*_{ijn} = 0$. We prove it by contradiction. Suppose that for certain $i_1, j_1 (> i_1), n_1$, we have $U^*_{i_1 j_1 n_1} = 0$ and $\Omega^*_{i_1 j_1 n_1} > 0$. Then we can create a new solution $(\mathbf{X}', \mathbf{Y}', \mathbf{U}', \mathbf{V}', \mathbf{\Omega}', \mathbf{s}', \mathbf{\Theta}', \mathbf{t}', \mathbf{\Gamma}', \mathbf{r}')$ by setting $s'_{i_1 j_1 n_1} = s^*_{i_1 j_1 n_1} + \Omega^*_{i_1 j_1 n_1}$, $\Omega'_{i_1 j_1 n_1} = 0$ and let all other variables be same as their counterparts in $(\mathbf{X}^*, \mathbf{Y}^*, \mathbf{U}^*, \mathbf{V}^*, \mathbf{\Omega}^*, \mathbf{s}^*, \mathbf{\Theta}^*, \mathbf{t}^*, \mathbf{\Gamma}^*, \mathbf{r}^*)$. It is easy to see that this new solution is feasible to *CptLinear* and

$$\Psi(\mathbf{X}^*, \mathbf{Y}^*, \mathbf{U}^*, \mathbf{V}^*, \mathbf{\Omega}^*, \mathbf{s}^*, \mathbf{\Theta}^*, \mathbf{t}^*, \mathbf{\Gamma}^*, \mathbf{r}^*) > \Psi(\mathbf{X}', \mathbf{Y}', \mathbf{U}', \mathbf{V}', \mathbf{\Omega}', \mathbf{s}', \mathbf{\Theta}', \mathbf{t}', \mathbf{\Gamma}', \mathbf{r}'),$$

which contradicts that $(\mathbf{X}^*, \mathbf{Y}^*, \mathbf{U}^*, \mathbf{V}^*, \mathbf{\Omega}^*, \mathbf{s}^*, \mathbf{\Theta}^*, \mathbf{t}^*, \mathbf{\Gamma}^*, \mathbf{r}^*)$ is an optimal solution.

Similarly, we can prove $\sum_i \sum_{j>i} \sum_n (\Theta^*_{ijn} - \sigma_{ij} V^*_{ijn}) = \sum_i \sum_{k\neq m} \sum_{m\neq j} \sum_{j>i} \sum_n F_{iknj} w_{ij} q_m X^*_{ikmj} V^*_{ijn}$, and $\sum_i \sum_{j>i} \sum_n (\Gamma^*_{ijn} - \sigma_{ij} U^*_{ijn}) = \sum_i \sum_{k\neq i,j} \sum_{j>i} \sum_n F_{innj} w_{ij} q_k X^*_{ikkj} U^*_{ijn}$. Therefore, we have

$$\Psi(\mathbf{X}^*, \mathbf{Y}^*, \mathbf{U}^*, \mathbf{V}^*, \mathbf{\Omega}^*, \mathbf{s}^*, \mathbf{\Theta}^*, \mathbf{t}^*, \mathbf{\Gamma}^*, \mathbf{r}^*) = \Phi(\mathbf{X}^*, \mathbf{Y}^*, \mathbf{U}^*, \mathbf{V}^*). \tag{18}$$

Next, we show that $(\mathbf{X}^*, \mathbf{Y}^*, \mathbf{U}^*, \mathbf{V}^*)$ is optimal to *R-SAHLP*. Again, we prove it by contradiction. Assume that there exists a feasible solution $(\mathbf{X}^0, \mathbf{Y}^0, \mathbf{U}^0, \mathbf{V}^0)$ to *R-SAHLP* such that

$$\Phi(\mathbf{X}^*, \mathbf{Y}^*, \mathbf{U}^*, \mathbf{V}^*) > \Phi(\mathbf{X}^0, \mathbf{Y}^0, \mathbf{U}^0, \mathbf{V}^0). \tag{19}$$

Then, we construct a feasible solution to *CptLinear* as follows.

For all $i, j > i, n$, if $\mathbf{U}^0_{ijn} = 1$, let $s^0_{ijn} = 0$ and $\Omega^0_{ijn} = \sum_{k\neq i} \sum_{m\neq k} F_{inmj} w_{ij} q_k X^*_{ikmj} + \sigma_{ij}$. Otherwise, let $s^0_{ijn} = \sum_{k\neq i} \sum_{m\neq k} F_{inmj} w_{ij} q_k X^*_{ikmj} + \sigma_{ij}$ and $\Omega^0_{ijn} = 0$. Note that both $\mathbf{\Omega}^0$ and $\mathbf{s}^0$ are nonnegative and they satisfy constraints in (11)-(12). We further assign nonnegative values to $\mathbf{\Theta}^0, \mathbf{t}^0, \mathbf{\Gamma}^0$ and $\mathbf{r}^0$ in a similar way. As a result, we obtain $(\mathbf{X}^0, \mathbf{Y}^0, \mathbf{U}^0, \mathbf{V}^0, \mathbf{\Omega}^0, \mathbf{s}^0, \mathbf{\Theta}^0, \mathbf{t}^0, \mathbf{\Gamma}^0, \mathbf{r}^0)$ as a feasible solution to *CptLinear*. In particular, we have $\Psi(\mathbf{X}^0, \mathbf{Y}^0, \mathbf{U}^0, \mathbf{V}^0, \mathbf{\Omega}^0, \mathbf{s}^0, \mathbf{\Theta}^0, \mathbf{t}^0, \mathbf{\Gamma}^0, \mathbf{r}^0) = \Phi(\mathbf{X^0}, \mathbf{Y^0}, \mathbf{U^0}, \mathbf{V^0})$. Clearly, because

(18) and (19), we have

$$\Psi(\mathbf{X}^*, \mathbf{Y}^*, \mathbf{U}^*, \mathbf{V}^*, \mathbf{\Omega}^*, \mathbf{s}^*, \mathbf{\Theta}^*, \mathbf{t}^*, \mathbf{\Gamma}^*, \mathbf{r}^*) > \Psi(\mathbf{X}^0, \mathbf{Y}^0, \mathbf{U}^0, \mathbf{V}^0, \mathbf{\Omega}^0, \mathbf{s}^0, \mathbf{\Theta}^0, \mathbf{t}^0, \mathbf{\Gamma}^0, \mathbf{r}^0),$$

which is the desired contradiction. □

Results in [6, 36, 22] show that applying this type of linearization techniques to a $0-1$ quadratic program will just linearly increase the number of variables and constraints. As *CptLinear* only has $O(|\mathbf{N}|^3)$ additional variables while the quadratic formula *R-SAHLP* has $O(|\mathbf{N}|^4)$ variables, it can be seen that, by appropriately utilizing problem structure, linearization may just add a few additional variables, which could be much less than those in the quadratic formula.

3.3 Lagrangian Relaxation and Branch-and-Bound

Existing professional mixed integer programming solvers can be applied to solve the linearized formulas. However, due to the large number of variables and constraints in the model, it may take excessive running times (see computational results in Table 1-4). Given that, we develop a Lagrangian relaxation algorithm that explores the structure of *R-SAHLP*. Comparing with other heuristic algorithms or commercial solvers, Lagrangian relaxation algorithm often yields high quality approximate or optimal solutions with much less computational time, see [35, 8]. Also, Branch-and-Bound methods are often implemented to identify an optimal solution if Lagrangian relaxation algorithm fails to obtain it. We next describe in details our algorithm development.

3.3.1 Lagrangian Lower Bound

For *R-SAHLP*, we dualize the constraints (2), (3), (4), (6) and (8) with $\alpha_{ijk,1}$, $\alpha_{ijm,2}$, β_i, $\gamma_{ijk,1} \geq 0$ and $\gamma_{ijm,2} \geq 0$ as their Lagrangian multipliers, respectively. As a result, we obtain the following relaxation where $\boldsymbol{\alpha}_1, \boldsymbol{\alpha}_2, \boldsymbol{\beta}, \boldsymbol{\gamma}_1$ and $\boldsymbol{\gamma}_2$ denote the corresponding

vectors for multipliers:

$$
\begin{aligned}
f(\boldsymbol{\alpha}_1, \boldsymbol{\alpha}_2, \boldsymbol{\beta}, \boldsymbol{\gamma}_1, \boldsymbol{\gamma}_2) = \min\ & \sum_i \sum_k \bar{C}_{ik} Y_{ik} - \sum_i \beta_i \\
& + \sum_i \sum_k \sum_m \sum_{j>i} (F_{ikmj} w_{ij} (1 - q_k - q_m^k) + \alpha_{ijk,1} + \gamma_{ijk,1} + \alpha_{ijm,2} + \gamma_{ijm,2}) X_{ikmj} \\
& + \sum_i \sum_{k \neq i} \sum_{m \neq k} \sum_{j>i} \sum_n F_{inmj} w_{ij} q_k X_{ikmj} U_{ijn} + \sum_i \sum_{j>i} \sum_k \gamma_{ijk,1} U_{ijk} \\
& + \sum_i \sum_{k \neq m} \sum_{m \neq j} \sum_{j>i} \sum_n F_{iknj} w_{ij} q_m X_{ikmj} V_{ijn} + \sum_i \sum_{j>i} \sum_m \gamma_{ijm,2} V_{ijm} \\
& + \sum_i \sum_{k \neq i,j} \sum_{j>i} \sum_n F_{innj} w_{ij} q_k X_{ikkj} U_{ijn} \qquad (20)
\end{aligned}
$$

subject to

$$
\begin{aligned}
& (5), (7), (9), (10) \\
& Y_{ik} \leq Y_{kk} \qquad \forall i, k \qquad (21)
\end{aligned}
$$

where

$$
\bar{C}_{ik} = \begin{cases} \beta_i - \sum_{j>i} \alpha_{ijk,1} - \sum_{j>i} \alpha_{jik,2}, & \text{if } i \neq k; \\ \beta_k + \sum_{i>k} (\phi_{ki} w_{ki} q_k - \alpha_{kik,1}) + \sum_{i<k} (\phi_{ik} w_{ik} q_k - \alpha_{ikk,2}) - \sum_i \sum_{j>i} (\gamma_{ijk,1} + \gamma_{ijk,2}), & \text{otherwise.} \end{cases}
$$

Note that (21) is implied in *R-SAHLP* and can be derived from (2) and (6). From the structure of (20) and the basic theory on Lagrangian multiplier, we obtain the next result, which allows us to apply classical subgradient method to obtain the strongest lower bound.

Corollary 3. *The function f defined in* (20) *is piece-wise linear and concave in* $(\boldsymbol{\alpha}_1, \boldsymbol{\alpha}_2, \boldsymbol{\beta}, \boldsymbol{\gamma}_1, \boldsymbol{\gamma}_2)$.

As a result, since $\mathbf{X}$ and $\mathbf{Y}$ variables are not linked anymore in the relaxed problem, it can be decomposed into two independent subproblems (**SAsub-1** and **SAsub-2**). Then, an optimal solution to the relaxed problem can be obtained by combining optimal solutions to these two problems together. The solution algorithms of the two subproblems are described next.

SAsub-1

$$
\min \{ \sum_i \sum_k \bar{C}_{ik} Y_{ik} - \sum_i \beta_i : \sum_k Y_{kk} = p, \ \ Y_{ik} \leq Y_{kk}\ \forall i, k,\ Y_{ik} \in \{0, 1\}\ \forall i, k. \}
$$

SAsub-1 is solved by a simple procedure as follows. Note that it can be completed within $O(|\mathbf{N}|^2)$.

Step 1: For each k, set $Y_{kk} = 1$. For i, k $(i \neq k)$, set $Y_{ik} = 1$ if $\bar{C}_{ik} < 0$ and $Y_{ik} = 0$ otherwise. Compute $S_k = \sum_i \bar{C}_{ik} Y_{ik}$, for each k.

Step 2: Sort S_k's in ascending order, choose smallest p S_k's and set the corresponding $Y_{kk} = 1$ and set the remaining Y_{kk}'s to 0. Calculate the optimal value of **SAsub-1** by $\sum_k S_k Y_{kk} - \sum_i \beta_i$.

Step 3: For i, k $(i \neq k)$, set Y_{ik} to 0 if $Y_{kk} = 0$.

SAsub-2

$$\begin{aligned}\min \sum_i \sum_k \sum_m \sum_{j>i} (F_{ikmj} w_{ij}(1 - q_k - q_m^k) + \alpha_{ijk,1} + \gamma_{ijk,1} + \alpha_{ijm,2} + \gamma_{ijm,2}) X_{ikmj} \\ + \sum_i \sum_{k \neq i} \sum_{m \neq k} \sum_{j>i} \sum_n F_{inmj} w_{ij} q_k X_{ikmj} U_{ijn} + \sum_i \sum_{j>i} \sum_k \gamma_{ijk,1} U_{ijk} \\ + \sum_i \sum_{k \neq m} \sum_{m \neq j} \sum_{j>i} \sum_n F_{iknj} w_{ij} q_m X_{ikmj} V_{ijn} + \sum_i \sum_{j>i} \sum_m \gamma_{ijm,2} V_{ijm} \\ + \sum_i \sum_{k \neq i,j} \sum_{j>i} \sum_n F_{innj} w_{ij} q_k X_{ikkj} U_{ijn}\end{aligned}$$

subject to

$$\sum_k \sum_m X_{ikmj} = 1 \qquad \forall i, j > i \tag{22}$$

$$U_{ijk} + \sum_m X_{ikmj} \leq 1 \qquad \forall i, j > i, k \tag{23}$$

$$\sum_k U_{ijk} = 1 - \sum_m X_{iimj} - \sum_m X_{ijmj} \qquad \forall i, j > i \tag{24}$$

$$V_{ijm} + \sum_k X_{ikmj} \leq 1 \qquad \forall i, j > i, m \tag{25}$$

$$\sum_m V_{ijm} = 1 - \sum_k X_{ikjj} - \sum_k X_{ikij} \qquad \forall i, j > i \tag{26}$$

$$X_{ikmj} \in \{0, 1\} \ \forall i, j > i, k, m; U_{ijk}, V_{ijk} \in \{0, 1\} \ \forall i, j > i, k \tag{27}$$

Constraints (22), (23) and (25) are redundant in the original model. Nevertheless, including them in **SAsub-2** yields solution that is more likely to be feasible to the original problem and therefore strengthens the lower bound obtained from Lagrangian relaxation. Note that all the constraints in (22)-(27) simply require that: each $i - j$ flow must have one regular route, and alternative route(s) unless its source or destination is a hub; regular hubs and backup hubs must be different. Also, from the objective function, we also observe that, if the regular route is a single-hub route, so is the alternative route. Furthermore, in **SAsub-2**, it is easy to see that an optimal solution for one $i - j$ flow, i.e. X_{ikmj}, U_{ijn} and V_{ijn},

is independent of those of others. So, it's sufficient to consider each individual $i-j$ flow with the following objective function and corresponding constraints from **SAsub-2**.

$$\begin{aligned}
&\sum_k \sum_m (F_{ikmj} w_{ij}(1-q_k-q_m^k) + \alpha_{ijk,1} + \gamma_{ijk,1} + \alpha_{ijm,2} + \gamma_{ijm,2}) X_{ikmj} \\
&+ \sum_{k\neq i} \sum_{m\neq k} \sum_n F_{inmj} w_{ij} q_k X_{ikmj} U_{ijn} + \sum_k \gamma_{ijk,1} U_{ijk} \\
&+ \sum_{k\neq m} \sum_{m\neq j} \sum_n F_{iknj} w_{ij} q_m X_{ikmj} V_{ijn} + \sum_m \gamma_{ijm,2} V_{ijm} \\
&+ \sum_{k\neq i,j} \sum_n F_{innj} w_{ij} q_k X_{ikkj} U_{ijn}
\end{aligned} \tag{28}$$

Although (28) is nonlinear, every feasible solution has a clear combinatorial structure. As shown in Figure 3.(a), if $i-j$ flow takes (i,k,m,j) as its regular route, a cost of $F_{ikmj} w_{ij}(1-q_k-q_m^k) + \alpha_{ijk,1} + \gamma_{ijk,1} + \alpha_{ijm,2} + \gamma_{ijm,2}$ will be incurred; if this flow takes n_u (n_v, respectively) as the backup hub for k (m, respectively), a cost of $F_{inmj} w_{ij} q_k + \gamma_{ijn_u,1}$ ($F_{iknj} w_{ij} V_{ijn} q_m + \gamma_{ijn_v,2}$, respectively) will be incurred additionally. Similar situation on transportation cost can be observed in Figure 3.(b) when $i-j$ flow selects a single-hub regular route. Such observations and constraints in (22)-(27) motivate us to develop the following enumeration procedure to identify an optimal solution to $i-j$ flow.

Step 1: For one pair of (k,m), i.e. a given regular route, obtain its best alternative route (or best backup hubs) by computing all possible backup hubs that are different from k and m and selecting the corresponding alternative routes (or a single alternative route if $k=m$) with the least transportation cost. Compute the total transportation costs from both the regular route and the alternative routes using (28).

Step 2: Repeat Step 1 for all (k,m) pairs and identify the pair that provides the least total transportation cost. Denote that pair by (k^*,m^*) and its corresponding best backup hubs by n_u^* and n_v^*.

Step 3: Obtain an optimal solution to (28) by setting $X_{ikmj}=1$ if $k=k^*$ and $m=m^*$, and otherwise to zero; setting $U_{ijn}=1$ if $n=n_u^*$, and otherwise to zero; setting $V_{ijn}=1$ if $n=n_v^*$, and otherwise to zero.

The computation complexity of this procedure for one $i-j$ flow is $O(|\mathbf{N}|^4)$ and therefore **SAsub-2** can be solved within $O(|\mathbf{N}|^6)$.

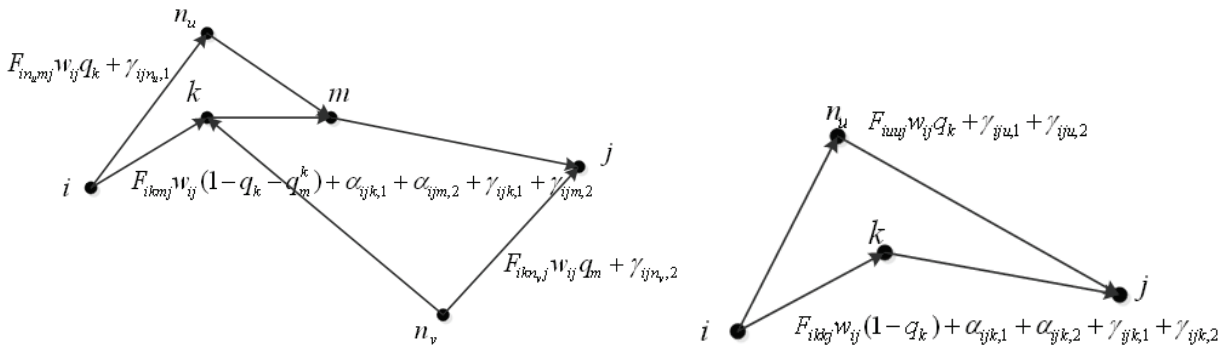

(a) A Two-hub Route and Its Alternative Routes (b) A Single-hub Route and Its Alternative Route

Figure 3: Transportation Cost of Solutions to **SAsub-2**

3.3.2 Upper Bound and Subgradient Method for Multiplier Updating

The solution procedure based on Lagrangian relaxation requires both a lower bound and an upper bound to the original problem. The value of the solution to the relaxation model provides a lower bound and the value of a feasible solution to the original problem yields an upper bound. To obtain a feasible solution, we apply a heuristic procedure that exploits the solution of **SAsub-1**. In [35], a similar heuristic (FEAS-2 in their paper) is implemented to the classical SA hub-and-spoke model and successfully achieves strong upper bounds. Specifically, for each node $i \in \mathbf{N}$, its allocation will be retained if (4) is not violated. For the node with allocation infeasible to (4), given that hubs are already fixed according to the solution to **SAsub-1**, we simply select the lowest cost allocation. After determining $\mathbf{Y}$ variables, the regular route for each $i-j$ flow is determined and its alternative routes can also be easily obtained by evaluating hubs not in the regular route and selecting the best ones.

With the lower bound and upper bound, we use the classical subgradient algorithm described in [18] to iteratively update the Lagrangian multipliers ($\boldsymbol{\alpha}_1, \boldsymbol{\alpha}_2, \boldsymbol{\beta}, \boldsymbol{\gamma}_1$ and $\boldsymbol{\gamma}_2$), and to search for the best lower bound. Specifically, at n-th iteration, we compute a step-size t^n as

$$t^n = \frac{\Delta^n (UB - LB^n)}{DM}$$

where

$$DM = \sum_i \sum_{j>i} \sum_k (\sum_m X_{ikmj} - Y_{ik})^2 + \sum_i \sum_{j>i} \sum_m (\sum_k X_{ikmj} - Y_{jm})^2 + \sum_i (\sum_k Y_{ik} - 1)^2 + \sum_i \sum_{j>i} \sum_k (U_{ijk} + \sum_m X_{ikmj} - Y_{kk})^2 + \sum_i \sum_{j>i} \sum_m (V_{ijm} + \sum_k X_{ikmj} - Y_{mm})^2,$$

Δ^n is n-th iteration step-size multiplier, UB is the best feasible solution (the one with the smallest objective value) ever found and LB^n is the lower bound obtained from n-th Lagrangian iteration. Multipliers are then updated by setting

$$\begin{aligned}
(\alpha_{ijk,1})^{n+1} &= (\alpha_{ijk,1})^n + t^n(\sum_m X_{ikmj} - Y_{ik}) \quad \forall i, j > i, k \\
(\alpha_{ijm,2})^{n+1} &= (\alpha_{ijm,2})^n + t^n(\sum_k X_{ikmj} - Y_{jm}) \quad \forall i, j > i, m \\
(\beta_i)^{n+1} &= (\beta_i)^n + t^n(\sum_k Y_{ik} - 1) \quad \forall i \\
(\gamma_{ijk,1})^{n+1} &= max\{(\gamma_{ijk,1})^n + t^n(U_{ijk} + \sum_m X_{ikmj} - Y_{kk}), 0\} \quad \forall i, j > i, k \\
(\gamma_{ijm,2})^{n+1} &= max\{(\gamma_{ijm,2})^n + t^n(V_{ijm} + \sum_k X_{ikmj} - Y_{mm}), 0\} \quad \forall i, j > i, m.
\end{aligned}$$

In all of our numerical study, parameter Δ^n is initialized to 6 and will be halved when 50 consecutive iterations fail to improve the lower bound with Lagrangian multipliers reset to the values used to obtain the best lower bound.

3.3.3 Variable Fixing

Variable fixing is an approach that uses both primal information from a feasible solution and dual information from Lagrangian multipliers to fix some variables in Lagrangian solution procedure. It has been proven to be effective in reducing search space and computation time, see [38, 8] for examples. In this section, we develop a few variable fixing rules to achieve this goal.

Assume that we have the current best upper bound UB, $(\boldsymbol{\alpha}_1, \boldsymbol{\alpha}_2, \boldsymbol{\beta}, \boldsymbol{\gamma}_1, \boldsymbol{\gamma}_2)$ are the current Lagrangian multipliers, and $(\mathbf{Y}^*, \mathbf{X}^*)$ is the corresponding optimal solution to the Lagrangian relaxed problem. Let $f(\boldsymbol{\alpha}_1, \boldsymbol{\alpha}_2, \boldsymbol{\beta}, \boldsymbol{\gamma}_1, \boldsymbol{\gamma}_2 | C)$ be the optimal objective function value for $(\boldsymbol{\alpha}_1, \boldsymbol{\alpha}_2, \boldsymbol{\beta}, \boldsymbol{\gamma}_1, \boldsymbol{\gamma}_2)$ under some condition C. Then, we have the following results.

Proposition 4. *When UB is strictly greater than LB,*
(i) if $Y^*_{kk} = 1$ and $f(\boldsymbol{\alpha}_1, \boldsymbol{\alpha}_2, \boldsymbol{\beta}, \boldsymbol{\gamma}_1, \boldsymbol{\gamma}_2 | Y_{kk} = 0) > UB$ for some k, we have $Y_{kk} = 1$ in any optimal solution;

(ii) if $Y^*_{kk} = 0$ *and* $f(\boldsymbol{\alpha}_1, \boldsymbol{\alpha}_2, \boldsymbol{\beta}, \boldsymbol{\gamma}_1, \boldsymbol{\gamma}_2 | Y_{kk} = 1) > UB$ *for some* k*, we have* $Y_{kk} = 0$ *in any optimal solution;*
(iii) if $Y^*_{ik} = 1$ *and* $f(\boldsymbol{\alpha}_1, \boldsymbol{\alpha}_2, \boldsymbol{\beta}, \boldsymbol{\gamma}_1, \boldsymbol{\gamma}_2 | Y_{ik} = 0) > UB$ *for some* i *and* k*, we have* $Y_{ik} = 1$*,* $Y_{kk} = 1$ *and* $Y_{im} = 0$ *for all* $m \neq k$ *in any optimal solution.*

Proof. We simply provide the proof for (i). Results in (ii) and (iii) can be proven using similar arguments.

Note that $f(\boldsymbol{\alpha}_1, \boldsymbol{\alpha}_2, \boldsymbol{\beta}, \boldsymbol{\gamma}_1, \boldsymbol{\gamma}_2 | Y_{kk} = 0)$ is a lower bound to *R-SAHLP* with a spoke located in node k for the given Lagrangian multipliers $(\boldsymbol{\alpha}_1, \boldsymbol{\alpha}_2, \boldsymbol{\beta}, \boldsymbol{\gamma}_1, \boldsymbol{\gamma}_2)$. So, if

$$f(\boldsymbol{\alpha}_1, \boldsymbol{\alpha}_2, \boldsymbol{\beta}, \boldsymbol{\gamma}_1, \boldsymbol{\gamma}_2 | Y_{kk} = 0) > UB,$$

any solution to *R-SAHLP* with a spoke in node k will generate more cost than the current best feasible solution. Therefore, we have $Y_{kk} = 1$ in any optimal solution to *R-SAHLP*. □

We mention that although more variable fixing rules can be developed, such as the case for $Y^*_{ik} = 0$, they will either be time consuming to implement or have less impact on the Lagrangian relaxation. We perform these variable fixing rules with the optimal multipliers once Lagrangian procedure is terminated. We note that the variable fixing procedure is quite effective in forcing variables open or closed and reducing gaps, similar to those observations made in [38, 8].

3.3.4 Branch-and-Bound Strategies

In this section, we first provide the termination conditions of Lagrangian relaxation algorithm and then describe a Branch-and-Bound framework through which we can obtain optimal solutions.

In the implementation of subgradient method, we terminate the Lagrangian procedure if one of the following conditions is met: (i) all Lagrangian multipliers are zero which implies the current solution is proven to be optimal; (ii) the difference between the upper and lower bounds is below a threshold value ϵ, i.e. an ϵ-optimal solution is found; (iii) the maximum number of iterations, Max_iter, is reached. For the last case, our Lagrangian relaxation algorithm discussed in the previous section will be embedded in a Branch-and-Bound framework to further reduce the gap between lower and upper bounds.

Branch-and-Bound technique with Lagrangian relaxation has been implemented in reliable facility location models [9, 38, 27]. Under some mild conditions, it is easy to prove that

once facilities are selected, all customers' assignments, including backup assignments, can be easily derived according to the relative distances between customers and facilities. Such a result implies that branching on facility location variables is sufficient for determining an optimal network structure [9, 38, 27]. However, this is not the case for *R-SAHLP*. Note that for a classical single allocation hub-and-spoke model, given fixed hubs, the remaining problem on spoke allocation has been proven to be NP-hard. Thus a more sophisticated Branch-and-Bound strategy must be developed to derive an optimal solution to *R-SAHLP*. To address this issue, we develop a two-stage Branch-and-Bound frame implemented in a width-first manner.

The first stage Branch-and-Bound is similar to that used for reliable facility location models in [38] where branching is made for Y_{kk} (hub location) variables. At each Branch-and-Bound node, the hub location variable $Y_{k^*k^*}$ selected for branching is the unfixed open hub with the greatest assigned flow (without considering alternative routes), i.e.

$$k^* = \arg\max_{k\in\mathbf{N}}\{\sum_i\sum_{j>i}\sum_m w_{ij}X_{ikmj} + \sum_i\sum_{j>i}\sum_{m\neq k} w_{ij}X_{imkj}\}.$$

$Y_{k^*k^*}$ is forced to be 0 and then 1. The first stage Branch-and-Bound process will be terminated either with an optimal (including ϵ-optimal) solution or with p hubs forced to open (or equivalently, $|\mathbf{N}| - p$ hubs forced to close).

In the latter case, we will apply the second stage Branch-and-Bound method to further reduce the gap and derive an optimal solution. In this stage, branching is made for Y_{ik} (allocation) variables for spoke i. We first, for nodes in the tree that need second stage Branch-and-Bound, compute the *level of violation*, v^i, for spoke i in the solution to Lagrangian relaxation. Specifically, given $(\tilde{X}, \tilde{Y}, \tilde{U}, \tilde{V})$, the current solution to Lagrangian relaxation, for spoke i, we calculate

$$v^i = |\mathbf{C}_1^i| + |\mathbf{C}_2^i| + I_i,$$

where

$$\mathbf{C}_1^i = \{(j,k)|\sum_m \tilde{X}_{ikmj} \neq \tilde{Y}_{ik}, j > i\},$$
$$\mathbf{C}_2^i = \{(j,k)|\sum_k \tilde{X}_{jkmi} \neq \tilde{Y}_{im}, j < i\},$$

and $I_i = 0$ if $\sum_k \tilde{Y}_{ik} = 1$, and $I_i = 1$ otherwise. Note that $|\mathbf{C}_1^i|$, $|\mathbf{C}_2^i|$, I_i represent the number of violations to constraints in (2), (3) and (4) for spoke i. Then, the spoke with the largest violation level v^i, say spoke i^*, will be selected for branching. Specifically, we

partition the hub set $\mathbf{H}$ (note that all hubs are already determined in the second stage Branch-and-Bound) into two sets $\mathbf{H}_1$ and $\mathbf{H}_2$ and create two nodes. We add constraint $\sum_{k\in\mathbf{H}_1} Y_{i^*k} = 1$ to the left hand node and add constraint $\sum_{k\in\mathbf{H}_2} Y_{i^*k} = 1$ to the right hand node. It can be easily seen that once hub and spoke allocation decisions are made, the remaining problem, including regular route and alternative route decisions, is polynomially solvable, which implies that no further branching is necessary.

The upper and lower bounds of a parent node will be updated whenever its child nodes are evaluated or updated. One node is fathomed if the gap between its upper and lower bounds is within ϵ and its child nodes will not be further evaluated. The best set of Lagrangian multipliers that yields the smallest gap at a given node will be passed to its child nodes and will be used as initial multipliers.

4 The Reliable Multiple Allocation Hub-and-spoke Model

In this section, we consider the reliable MA-HLP model, denoted by *R-MAHLP*. Similar to our study on *R-SAHLP*, we first provide the mathematical formulation, analyze its complexity and then describe our solution strategy using Lagrangian relaxation method and a Branch-and-Bound framework.

4.1 Reliable MA Model: Definition and Formulation

Compared with the single allocation model, the multiple allocation model does not restrict flows from the same source (or to the same destination) route through same hubs. This relaxation provides a freedom such that each flow can make its route decision independent of other flows. As a result, we do not need to introduce variables to denote spoke-hub allocations but simply introduce binary variables to define hubs. In the following, we provide the formulation for *R-MAHLP*. As most constraints reflect the requirements similar to those in *R-SAHLP*, we simply provide a brief explanation to new constraints.

$\underline{R-MAHLP}$

$$\begin{aligned}\min\ & \sum_i \sum_k \sum_m \sum_{j>i} F_{ikmj} w_{ij} (1 - q_k - q_m^k) X_{ikmj} \\ & + \sum_i \sum_{k\neq i} \sum_{m\neq k} \sum_{j>i} \sum_n F_{inmj} w_{ij} q_k X_{ikmj} U_{ijn} \\ & + \sum_i \sum_{k\neq m} \sum_{m\neq j} \sum_{j>i} \sum_n F_{iknj} w_{ij} q_m X_{ikmj} V_{ijn} \\ & + \sum_i \sum_{k\neq i,j} \sum_{j>i} \sum_n F_{innj} w_{ij} q_k X_{ikkj} U_{ijn} + \sum_i \sum_{j>i} \phi_{ij} w_{ij} (q_i Y_i + q_j Y_j)\end{aligned}$$

subject to

$$\sum_k X_{ikjj} = Y_j \qquad \forall i, j > i \tag{29}$$

$$\sum_m X_{iimj} = Y_i \qquad \forall i, j > i \tag{30}$$

$$\sum_i Y_i = p \tag{31}$$

$$\sum_k \sum_m X_{ikmj} = 1 \qquad \forall i, j > i \tag{32}$$

$$U_{ijk} + \sum_m X_{ikmj} \leq Y_k \qquad \forall i, j > i, k \tag{33}$$

$$\sum_k U_{ijk} = 1 - \sum_m X_{iimj} - \sum_m X_{ijmj} \qquad \forall i, j > i \tag{34}$$

$$V_{ijm} + \sum_k X_{ikmj} \leq Y_m \qquad \forall i, j > i, m \tag{35}$$

$$\sum_m V_{ijm} = 1 - \sum_k X_{ikjj} - \sum_k X_{ikij} \qquad \forall i, j > i \tag{36}$$

$$X_{ikmj} \in \{0,1\}\ \forall i, j > i, k, m;\ Y_k \in \{0,1\}\ \forall k;\ U_{ijk}, V_{ijk} \in \{0,1\}\ \forall i, j > i, k \tag{37}$$

We use a binary variable Y_k to indicate whether k is a hub. Constraints (29)-(30) simply imply that if i (or j) is a hub, it must be the first (or the second) hub in the routes of all flows from i (or to j). Constraints (32) require that each $i-j$ flow must have a route through hub(s).

Compared to the *R-SAHLP*, *R-MAHLP* is much simpler. First, as [4] states that, for the classical *MA-HLP*, since there is no capacity restriction on links, each $i-j$ flow should be routed through the least-cost hub pair. As a result, one optimal solution would always force the X variables to be 1 or 0 and therefore there is no need to restrict X variables to be binary. Second, it is easy to observe that, if p is fixed, *MA-HLP* is polynomial solvable. In fact, these two observations hold in *R-MAHLP*.

Proposition 5. *For a given p, the R-MAHLP problem is a polynomial solvable and there exists one optimal solution such that all the flow variables X_{ikmj} take either 0 or 1 for all $i, j > i, k$ and m.*

In the next section, we describe a Lagrangian relaxation based solution procedure as well as a Branch-and-Bound scheme to solve the *R-MAHLP* efficiently. Because the solution procedure is similar to that of *R-SAHLP*, we only provide necessary descriptions to minimize the redundancy.

4.2 Solution Methods for *R-MAHLP*

Note that the two reformulation approaches described in Section 3.2 could be applied to *R-MAHLP* with little modification. So, we just describe the development of Lagrangian relaxation algorithm for *R-MAHLP*. We dualize constraints linking the route variables **X** and the hub variables **Y** and solve two resulting subproblems separately. By dualizing constraints in (29), (30), (33) and (35) with Lagrangian multipliers $\alpha_{ij,1}$, $\alpha_{ij,2}$, $\gamma_{ijk,1} \geq 0$ and $\gamma_{ijm,2} \geq 0$, we obtain subproblems **MAsub-1** and **MAsub-2** as follows.

MAsub-1

$$\min\{\sum_k \bar{C}_k Y_k : \sum_k Y_k = p, \quad Y_k \in \{0,1\}\ \forall k\}$$

where $\bar{C}_k = \sum_{i<k}(\phi_{ik} w_{ik} q_k - \alpha_{ik,1}) + \sum_{i>k}(\phi_{ki} w_{ki} q_k - \alpha_{ki,2}) - \sum_i \sum_{j>i}(\gamma_{ijk,1} + \gamma_{ijk,2})$. Clearly, **MAsub-1** can be solved by sorting variables according to their coefficients and selecting the smallest p of them.

MAsub-2

$$\begin{aligned}
\min\ & \sum_i \sum_k \sum_m \sum_{j>i} (F_{ikmj} w_{ij}(1 - q_k - q_m^k) + \gamma_{ijk,1} + \gamma_{ijm,2}) X_{ikmj} \\
& + \sum_i \sum_{j>i} \sum_k \alpha_{ij,1} X_{ikjj} + \sum_i \sum_{j>i} \sum_m \alpha_{ij,2} X_{iimj} \\
& + \sum_i \sum_{k\neq i} \sum_{m\neq k} \sum_{j>i} \sum_n F_{inmj} w_{ij} q_k X_{ikmj} U_{ijn} \\
& + \sum_i \sum_{k\neq m} \sum_{m\neq j} \sum_{j>i} \sum_n F_{iknj} w_{ij} q_m X_{ikmj} V_{ijn} \\
& + \sum_i \sum_{k\neq i,j} \sum_{j>i} \sum_n F_{innj} w_{ij} q_k X_{ikkj} U_{ijn} + \sum_i \sum_{j>i} \sum_k (\gamma_{ijk,1} U_{ijk} + \gamma_{ijk,2} V_{ijk})
\end{aligned}$$

subject to

$$(32), (34), (36), (37)$$

$$U_{ijk} + \sum_{m} X_{ikmj} \leq 1 \qquad \forall i, j > i, k \tag{38}$$

$$V_{ijm} + \sum_{k} X_{ikmj} \leq 1 \qquad \forall i, j > i, m \tag{39}$$

Similar to **SAsub-2**, constraints (38) and (39) are supplied to get a tighter lower bound. Again, we can simply consider every single $i - j$ flow and combine solution from every flow to obtain an overall optimal solution. In fact, similar to **SAsub-2** of *R-SAHLP*, **MAsub-2** can also be interpreted using its combinatorial structure with appropriate cost coefficients and solved by a enumeration procedure. To obtain a feasible solution, as well as an upper bound, we follow the result from **MAsub-1** to fix hubs. Then, an optimal solution for those given hubs can be determined by deriving optimal route for each individual $i - j$ flow.

We update Lagrangian multipliers iteratively by applying classical subgradient algorithm to obtain the strongest lower bound and derive the best upper bound accordingly. Also, a variable fixing strategy, which just considers hub location variables, is developed and implemented. In case that one optimal (including ϵ-optimal) solution cannot be obtained, a Branch-and-Bound technique, similar to that of *R-SAHLP*, is implemented to reduce the gap. Given that optimal routing decisions can be obtained in polynomial time if all hubs are fixed, this Branch-and-Bound procedure is guaranteed to be completed by branching on hub location variables only, which has a similar complexity to that of reliable facility location models in [38, 27, 9]

5 Computational Experiments

In this section, the numerical study of the developed solution algorithms is presented. We first describe the testing data and experiment setup. Then, we provide computational results obtained from a professional solver and the Lagrangian relaxation/Branch-and-Bound algorithms on various instances. We also discuss the impact of reliable models on system design and operations to gain insights.

5.1 Data and Design of Experiments

We test our algorithms on the widely used CAB data set [32]. CAB data set contains distance/cost and traffic flow information, i.e. $\mathbf{c}$ and $\mathbf{w}$, among 25 US major cities (i.e. 25 nodes in our model) in 1970s. To consider the impact of unavailability, we investigate two scenarios of unavailability $\mathbf{q}$. In the first scenario, q_i is randomly selected from interval $(0, 0.1)$ for all $i \in \mathbf{N}$ to represent the environment with low unavailability. In the second scenario, q_i is randomly selected from $(0.2, 0.3)$ for all $i \in \mathbf{N}$ to represent the high unavailability environment. In each scenario, we consider thirty six n, p and γ combinations: $n = 10, 15, 20, 25$; $p = 3, 5, 7$ and $\gamma = 0.3, 0.5, 0.7$. So, we have two groups of 36 instances, denoted by *HLPl* for low and *HLPh* for high unavailability scenario respectively.

The aforementioned instances provide a testbed for both *R-SAHLP* and *R-MAHLP* models. We set the optimality tolerance to 1% for all solution methods, including the off-the-shelf MIP solver CPLEX 12.1. For Lagrangian relaxation/Branch-and-Bound algorithm, we follow the most setup used in [35]. The initial values of all multipliers are set to zero. Δ, the step-size multiplier is set to 6; the maximum number of iterations allowed before an improvement in the lower bound is set to 50; the maximum number of iterations at the root node in the branch-and-bound tree is set to 3000 and at a child node it is set to 200. For CPLEX, except the optimality tolerance, we adopt its default settings in all computational experiments to explore two linearized models, i.e. *StdLinear* and *CptLinear*. For both Lagrangian relaxation/Branch-and-Bound algorithm and CPLEX, we set the computation time limit to 1800 seconds CPU time. If some instance cannot be solved due to time limit or memory issue, we use T and M to represent the reason.

All algorithms are implemented in C++ and all instances are tested on a Dell Optiplex 760 desktop computer (Intel Core 2 Duo CPU, 3.0GHz, 3.25GB of RAM) in Windows XP environment.

5.2 Performance of Different Linearization Methods

We solve all instances by calling CPLEX 12.1 using linearization models *StdLinear* and *CptLinear*. Since [22] mention that the values of σ_{ij} could affect the performance of MIP solver, we solve *CptLinear* with $\boldsymbol{\sigma} = \mathbf{0}$ and $\boldsymbol{\sigma} = 0.6\boldsymbol{\mu}$. Computational results are presented in Table 1-2 for low and high unavailability situation respectively. CPLEX results for *R-MAHLP* are listed in Table 3-4. For the case CPLEX 12.1 can not find an optimal

solution, the table will show the best feasible solution followed by the corresponding gap (in percentage) in the brackets.

By checking the performance of *StdLinear* and *CptLinear* models for various instances, we observe that: (*i*) both models work better for instances with low unavailability than for high unavailability instances, which also agrees with the observation made on Lagrangian relaxation/Branch-and-Bound. So, it indicates the new challenges in algorithm design brought by probability and reliability. We provide detailed analysis in Section 5.3 as most instances are not solved by CPLEX and therefore less structural information can be obtained; (*ii*) *StdLinear* model is only suitable for small size instances, which can be explained by the huge number of variables and constraints it brings; (*iii*) *CptLinear* is comparable with *StdLinear* for small instances but is definitely better than *StdLinear* for larger instances. However, it often fails to generate optimal solutions within the time limit as this model typically has a large gap with its linear programming relaxation; (*iv*) *CptLinear* performs differently with different parameter values of $\boldsymbol{\sigma}$. Generally, the smaller values for parameter $\boldsymbol{\sigma}$, the less gap between lower and upper bounds before terminations. This observation is different from that obtained in [22] which notes that larger $\boldsymbol{\sigma}$ could lead to better performance on the compact formula for classical single allocation instances. We believe that more research needs to be done on how to fine tune $\boldsymbol{\sigma}$ to achieve the optimal performance.

Overall, linearized models with CPLEX is not an efficient solution strategy for reliable hub-and-spoke models. Efficient algorithms, such as our Lagrangian relaxation/Branch-and-Bound method, are necessary to solve instances of practical sizes.

5.3 Performance of Lagrangian Relaxation and Branch-and-Bound

Table 5-6 summarize the computational results of our Lagrangian relaxation and Branch-and-Bound methods for instances of *R-SAHLPl* and *R-SAHLPh* and Table 7-8 list the results for *R-MAHLPl* and *R-MAHLPh*. Column marked *#Lagiter.* indicates the number of Lagrangian iterations in all Branch-and-Bound nodes; column marked *Gap(%)* provides the smallest relative gap we have achieved before termination of Lagrangian relaxation algorithm; column *BB-1* shows the number of nodes (in addition to the root node) in the first stage Branch-and-Bound; column *BB-2* indicates the number of nodes in the second stage Branch-and-Bound; column marked *Time(s)* presents the total computational time in seconds.

Table 1: CPLEX performance for *R-SAHLPl* with $\mathbf{q} \in (0, 0.1)$

$\|\mathbf{N}\|$	p	γ	*StdLinear*		*CptLinear* ($\boldsymbol{\sigma} = \mathbf{0}$)		*CptLinear* ($\boldsymbol{\sigma} = 0.6\boldsymbol{\mu}$)	
			Time(s)	*obj.* ($\times 10^6$)	*Time(s)*	*obj.* ($\times 10^6$)	*Time(s)*	*obj.* ($\times 10^6$)
10	3	0.3	20.8	274.863	14.8	274.863	T	274.863 (9.33)
	5	0.3	8.9	208.385	2.1	208.781	T	208.385 (2.40)
	7	0.3	4.1	168.223	1.4	168.465	38.3	168.819
	3	0.5	33.9	311.335	4.5	311.420	T	311.335 (6.86)
	5	0.5	24.5	256.437	5.5	256.633	T	256.437 (10.63)
	7	0.5	9.4	222.835	6.6	223.583	36.6	223.470
	3	0.7	42.6	347.781	35.0	347.913	T	347.864 (8.16)
	5	0.7	26.6	300.087	14.3	299.866	T	299.250 (9.41)
	7	0.7	16.5	277.419	10.6	277.011	52.2	276.797
15	3	0.3	M	NA	T	1086.820 (8.05)	T	1086.820 (10.20)
	5	0.3	M	NA	T	830.509 (5.88)	T	830.509 (7.50)
	7	0.3	M	NA	T	701.034 (3.79)	T	701.034 (4.81)
	3	0.5	M	NA	T	1209.620 (7.20)	T	1209.620 (11.36)
	5	0.5	M	NA	T	988.629 (5.63)	T	989.227 (7.27)
	7	0.5	M	NA	T	872.283 (3.15)	T	872.603 (4.43)
	3	0.7	M	NA	T	1320.800 (8.26)	T	1329.930 (13.05)
	5	0.7	M	NA	T	1148.150 (6.54)	T	1148.170 (8.17)
	7	0.7	M	NA	T	1046.060 (4.14)	T	1046.060 (5.57)
20	3	0.3	M	NA	T	NA	T	2694.160 (92.51)
	5	0.3	M	NA	M	NA	T	2009.630 (104.02)
	7	0.3	M	NA	T	1574.570 (7.51)	T	1571.610 (7.90)
	3	0.5	M	NA	T	NA	T	2831.020 (89.21)
	5	0.5	M	NA	M	NA	T	2543.910 (96.93)
	7	0.5	M	NA	T	1978.610 (6.46)	M	NA
	3	0.7	M	NA	T	NA	T	3114.930 (90.50)
	5	0.7	M	NA	T	2720.850 (12.07)	T	2951.460 (94.39)
	7	0.7	M	NA	T	2440.550 (8.83)	T	2524.220 (12.07)
25	3	0.3	M	NA	T	NA	T	NA
	5	0.3	M	NA	T	NA	T	NA
	7	0.3	M	NA	T	NA	T	NA
	3	0.5	M	NA	T	NA	T	NA
	5	0.5	M	NA	T	NA	T	NA
	7	0.5	M	NA	T	NA	T	NA
	3	0.7	M	NA	T	NA	T	NA
	5	0.7	M	NA	T	NA	T	NA
	7	0.7	M	NA	T	NA	T	NA

Table 2: CPLEX performance for *R-SAHLPh* with $\mathbf{q} \in (0.2, 0.3)$

$\|\mathbf{N}\|$	p	γ	*StdLinear*		*CptLinear* ($\boldsymbol{\sigma} = \mathbf{0}$)		*CptLinear* ($\boldsymbol{\sigma} = 0.6\boldsymbol{\mu}$)	
			Time(s)	*obj.* ($\times 10^6$)	*Time(s)*	*obj.* ($\times 10^6$)	*Time(s)*	*obj.* ($\times 10^6$)
10	3	0.3	T	347.628 (20.59)	T	347.628 (24.69)	T	364.134 (51.61)
	5	0.3	T	321.611 (12.83)	T	323.286 (19.16)	T	321.611 (35.61)
	7	0.3	335.1	321.228	T	321.228 (8.40)	T	321.228 (12.33)
	3	0.5	T	371.287 (21.19)	T	371.287 (22.09)	T	378.850 (56.65)
	5	0.5	T	352.486 (16.66)	T	352.486 (20.84)	T	362.634 (42.63)
	7	0.5	343.1	352.195	T	352.195 (10.90)	T	354.645 (13.63)
	3	0.7	T	392.205 (21.32)	T	397.925 (23.98)	T	392.205 (50.25)
	5	0.7	T	380.172 (16.45)	T	380.516 (19.28)	T	391.306 (37.80)
	7	0.7	421.5	382.657	T	384.268 (11.47)	T	387.760 (12.51)
15	3	0.3	M	NA	T	1325.220 (41.55)	T	1439.920 (73.22)
	5	0.3	M	NA	T	1221.040 (41.56)	T	1220.110 (44.12)
	7	0.3	M	NA	T	1113.310 (33.77)	T	1130.810 (36.51)
	3	0.5	M	NA	T	1410.770 (42.84)	T	1559.290 (79.53)
	5	0.5	M	NA	T	1309.470 (40.97)	T	1330.880 (51.15)
	7	0.5	M	NA	T	1219.630 (34.68)	T	1219.630 (35.54)
	3	0.7	M	NA	T	1493.560 (43.38)	T	1644.600 (81.21)
	5	0.7	M	NA	T	1384.150 (39.93)	T	1378.370 (45.26)
	7	0.7	M	NA	T	1296.640 (33.28)	T	1296.140 (34.55)
20	3	0.3	M	NA	T	NA	T	3349.270 (247.06)
	5	0.3	M	NA	T	3666.980 (63.57)	T	3014.640 (258.05)
	7	0.3	M	NA	T	2408.800 (43.90)	T	2613.880 (271.31)
	3	0.5	M	NA	T	NA	T	3600.720 (248.39)
	5	0.5	M	NA	T	3605.790 (58.76)	T	3067.120 (266.41)
	7	0.5	M	NA	T	2767.990 (45.10)	T	2979.090 (258.21)
	3	0.7	M	NA	T	NA	T	4006.810 (248.91)
	5	0.7	M	NA	T	3193.240 (48.67)	T	3443.830 (263.08)
	7	0.7	M	NA	T	3255.110 (48.57)	T	3006.130 (271.17)
25	3	0.3	M	NA	T	NA	T	NA
	5	0.3	M	NA	T	NA	T	NA
	7	0.3	M	NA	T	NA	T	NA
	3	0.5	M	NA	T	NA	T	NA
	5	0.5	M	NA	T	NA	T	NA
	7	0.5	M	NA	T	NA	T	NA
	3	0.7	M	NA	T	NA	T	NA
	5	0.7	M	NA	T	NA	T	NA
	7	0.7	M	NA	T	NA	T	NA

Table 3: CPLEX performance for *R-MAHLPl* with $\mathbf{q} \in (0, 0.1)$

$\|\mathbf{N}\|$	p	γ	*StdLinear*		*CptLinear* ($\boldsymbol{\sigma} = \mathbf{0}$)		*CptLinear* ($\boldsymbol{\sigma} = 0.6\boldsymbol{\mu}$)	
			Time(s)	*obj.* ($\times 10^6$)	*Time(s)*	*obj.* ($\times 10^6$)	*Time(s)*	*obj.* ($\times 10^6$)
10	3	0.3	9.5	270.246	14.1	269.219	T	269.219 (29.02)
	5	0.3	2.9	202.130	1.5	202.082	70.1	201.835
	7	0.3	2.8	166.800	1.4	166.848	25.3	167.256
	3	0.5	4.2	293.175	2.1	292.610	T	292.333 (27.21)
	5	0.5	2.4	244.422	0.4	244.022	419.9	244.371
	7	0.5	2.3	219.088	0.6	219.047	23.2	219.426
	3	0.7	4.4	312.116	3.5	311.639	T	311.633 (17.97)
	5	0.7	4.7	283.598	1.7	283.283	81.1	283.031
	7	0.7	3.1	267.830	1.3	267.562	34.7	267.310
15	3	0.3	M	NA	T	1067.960 (7.34)	T	1119.140 (490.42)
	5	0.3	M	NA	T	813.889 (6.11)	T	849.649 (499.35)
	7	0.3	M	NA	T	687.874 (3.68)	T	779.923 (455.52)
	3	0.5	M	NA	T	1168.040 (6.91)	T	1268.620 (492.64)
	5	0.5	M	NA	T	942.792 (5.20)	T	1083.190 (511.78)
	7	0.5	M	NA	T	840.832 (3.14)	T	901.123 (504.82)
	3	0.7	M	NA	T	1233.550 (6.02)	T	1305.880 (526.45)
	5	0.7	M	NA	T	1064.010 (4.96)	T	1074.840 (532.09)
	7	0.7	M	NA	T	994.186 (3.75)	T	1034.970 (438.23)
20	3	0.3	M	NA	T	2418.190 (8.33)	T	2915.340 (644.37)
	5	0.3	M	NA	T	1764.060 (6.10)	T	2241.920 (766.61)
	7	0.3	M	NA	T	1537.540 (6.69)	T	1968.310 (800.99)
	3	0.5	M	NA	T	2613.500 (8.16)	T	3019.950 (608.97)
	5	0.5	M	NA	T	2114.380 (7.13)	T	2443.610 (721.94)
	7	0.5	M	NA	T	1907.070 (6.53)	T	2404.180 (662.58)
	3	0.7	M	NA	T	2784.510 (7.77)	T	3257.380 (708.73)
	5	0.7	M	NA	T	2453.740 (8.67)	T	2757.580 (662.33)
	7	0.7	M	NA	T	2258.920 (6.98)	T	2691.680 (589.53)
25	3	0.3	M	NA	M	NA	M	NA
	5	0.3	M	NA	M	NA	M	NA
	7	0.3	M	NA	M	NA	M	NA
	3	0.5	M	NA	M	NA	M	NA
	5	0.5	M	NA	M	NA	M	NA
	7	0.5	M	NA	M	NA	M	NA
	3	0.7	M	NA	M	NA	M	NA
	5	0.7	M	NA	M	NA	M	NA
	7	0.7	M	NA	M	NA	M	NA

Table 4: CPLEX performance for *R-MAHLPh* with $\mathbf{q} \in (0.2, 0.3)$

$\|\mathbf{N}\|$	p	γ	*StdLinear*		*CptLinear* ($\boldsymbol{\sigma} = \mathbf{0}$)		*CptLinear* ($\boldsymbol{\sigma} = 0.6\boldsymbol{\mu}$)	
			Time(s)	*obj.* ($\times 10^6$)	*Time(s)*	*obj.* ($\times 10^6$)	*Time(s)*	*obj.* ($\times 10^6$)
10	3	0.3	T	380.413 (36.85)	T	346.754 (21.43)	T	346.754 (56.48)
	5	0.3	T	330.750 (22.93)	T	321.053 (18.70)	T	325.301 (45.46)
	7	0.3	T	321.228 (7.05)	T	322.024 (8.23)	T	322.024 (19.48)
	3	0.5	T	379.523 (30.42)	T	366.266 (22.13)	T	366.266 (53.29)
	5	0.5	T	355.215 (21.79)	T	348.792 (18.77)	T	348.792 (50.33)
	7	0.5	T	352.263 (10.44)	T	352.263 (11.28)	T	352.263 (18.58)
	3	0.7	T	389.372 (28.11)	T	376.730 (21.71)	T	376.730 (49.54)
	5	0.7	T	372.982 (20.64)	T	366.847 (17.15)	T	372.339 (51.58)
	7	0.7	T	376.189 (8.62)	T	376.189 (11.12)	T	376.189 (22.80)
15	3	0.3	M	NA	T	1362.960 (45.21)	T	1355.380 (551.71)
	5	0.3	M	NA	T	1174.740 (40.41)	T	1164.100 (291.95)
	7	0.3	M	NA	T	1118.570 (35.39)	T	1154.200 (306.78)
	3	0.5	M	NA	T	1386.690 (43.22)	T	1422.820 (528.38)
	5	0.5	M	NA	T	1251.700 (39.45)	T	1271.580 (320.71)
	7	0.5	M	NA	T	1192.310 (34.28)	T	1212.730 (345.99)
	3	0.7	M	NA	T	1433.440 (42.44)	T	1475.270 (538.70)
	5	0.7	M	NA	T	1290.650 (36.87)	T	1345.340 (419.85)
	7	0.7	M	NA	T	1260.650 (33.47)	T	1266.850 (288.68)
20	3	0.3	M	NA	T	3191.260 (53.15)	T	3285.030 (646.86)
	5	0.3	M	NA	T	2582.690 (48.80)	T	2922.410 (646.93)
	7	0.3	M	NA	T	2344.880 (43.52)	T	2635.250 (657.89)
	3	0.5	M	NA	T	3329.830 (51.49)	T	3509.320 (658.21)
	5	0.5	M	NA	T	2761.560 (47.28)	T	3161.650 (654.62)
	7	0.5	M	NA	T	2655.890 (44.35)	T	2817.950 (681.69)
	3	0.7	M	NA	T	3403.370 (49.95)	T	3756.750 (690.33)
	5	0.7	M	NA	T	2920.230 (46.34)	T	3264.620 (665.62)
	7	0.7	M	NA	T	2839.850 (43.76)	T	3150.920 (529.95)
25	3	0.3	M	NA	M	NA	M	NA
	5	0.3	M	NA	M	NA	M	NA
	7	0.3	M	NA	M	NA	M	NA
	3	0.5	M	NA	M	NA	M	NA
	5	0.5	M	NA	M	NA	M	NA
	7	0.5	M	NA	M	NA	M	NA
	3	0.7	M	NA	M	NA	M	NA
	5	0.7	M	NA	M	NA	M	NA
	7	0.7	M	NA	M	NA	M	NA

We observe from those tables that: (i) the Lagrangian algorithm with Branch-and-Bound is very efficient in solving reliable models. All 144 instances can be solved to optimality within 1800s; (ii) in general, the Lagrangian algorithm itself could produce sufficiently tight bounds at the root node. Among all instances, 97.2% (80.6%, 100% and 75%, respectively) of the *R-SAHLPl*(*R-SAHLPh*, *R-MAHLPl* and *R-MAHLPh*, respectively) are solved at their root nodes; (iii) Branch-and-Bound technique is necessary to derive optimal solutions for quite a few instances. This observation clearly shows that reliable models are more challenging than the classical ones, such as those studied in [35]. Furthermore, instances with low availability, i.e. $\mathbf{q}$ is high, are more difficult to compute than those with high availability, and instances with small number of hubs are more challenging than those with large number of hubs. Those two observations are linked with the critical role of hubs. When hubs are less available, the structure of reliable hub-and-spoke model will be less similar to classical models as more interactions between regular and backup hubs are included in solution space. So, algorithms must demand more computational efforts to identify optimal solutions. The latter one can be explained by the fact that when the number of hubs is large, it would be close to optimal by simply allocating spokes to their nearest hubs, which is exactly the logic behind the heuristic algorithms for feasible solutions.

5.4 Analysis and Discussion on System Design and Performance

In this section, we discuss the impact of reliable design paradigm on the system configuration and transportation performance measures. The performance measures include the number of passengers transported successfully (denoted by *Psg*), the mileage (denoted by *Mileage*) and the cost (denoted by *Cost*) of the whole network.

Throughout this section, we use the network configuration determined by a classical hub-and-spoke model, which actually is a special case of *R-SAHLP* or *R-MAHLP* if we ignore hub availability, as a benchmark. The performance measures under the environment with unavailability are computed as follows. Note that we include the term q_k and q_m^k to precisely capture the real situation under the assumption of independent hub unavailability.

$$Psg = \sum_i \sum_k \sum_m \sum_{j>i} w_{ij}(1 - q_k - q_m^k + q_k q_m^k) X_{ikmj},$$

$$Mileage = \sum_i \sum_k \sum_m \sum_{j>i} (c_{ik} + c_{km} + c_{mj}) w_{ij}(1 - q_k - q_m^k + q_k q_m^k) X_{ikmj},$$

$$Cost = \sum_i \sum_k \sum_m \sum_{j>i} F_{ikmj} w_{ij}(1 - q_k - q_m^k + q_k q_m^k) X_{ikmj}.$$

Similarly, we calculate the system performance of the reliable hub-and-spoke network,

Table 5: LR and Branch-and-Bound for *R-SAHLPl* with $\mathbf{q} \in (0, 0.1)$

$\|\mathbf{N}\|$	p	γ	$\#Lagiter.$	$Gap(\%)$	$BB-1$	$BB-2$	$BB-Gap(\%)$	$Time(s)$
10	3	0.3	383	0.000	0	0	-	0.8
	5	0.3	458	0.006	0	0	-	0.9
	7	0.3	288	0.064	0	0	-	0.6
	3	0.5	395	0.004	0	0	-	0.7
	5	0.5	426	0.014	0	0	-	1.4
	7	0.5	317	0.191	0	0	-	1.2
	3	0.7	252	0.973	0	0	-	0.9
	5	0.7	315	0.030	0	0	-	1.2
	7	0.7	298	0.274	0	0	-	0.6
15	3	0.3	994	0.730	0	0	-	14.4
	5	0.3	353	0.010	0	0	-	6.9
	7	0.3	427	0.174	0	0	-	8.1
	3	0.5	958	0.601	0	0	-	13.8
	5	0.5	401	0.389	0	0	-	9.8
	7	0.5	373	0.229	0	0	-	8.1
	3	0.7	766	0.982	0	0	-	9.5
	5	0.7	251	0.961	0	0	-	4.3
	7	0.7	474	0.731	0	0	-	10.7
20	3	0.3	874	0.579	0	0	-	51.4
	5	0.3	413	0.092	0	0	-	31.2
	7	0.3	431	0.301	0	0	-	29.1
	3	0.5	1139	0.635	0	0	-	61.0
	5	0.5	566	0.267	0	0	-	38.0
	7	0.5	413	0.676	0	0	-	35.9
	3	0.7	901	0.951	0	0	-	43.7
	5	0.7	639	0.966	0	0	-	31.7
	7	0.7	661	0.775	0	0	-	46.9
25	3	0.3	1312	0.702	0	0	-	209.4
	5	0.3	382	0.737	0	0	-	59.6
	7	0.3	240	0.930	0	0	-	39.2
	3	0.5	1363	0.902	0	0	-	224.9
	5	0.5	548	0.247	0	0	-	124.5
	7	0.5	300	0.964	0	0	-	46.7
	3	0.7	3486	1.030	2	0	0.905	458.8
	5	0.7	445	0.995	0	0	-	66.0
	7	0.7	427	0.982	0	0	-	63.9

Table 6: LR and Branch-and-Bound for *R-SAHLPh* with $\mathbf{q} \in (0.2, 0.3)$

$\|\mathbf{N}\|$	p	γ	$\#Lagiter.$	$Gap(\%)$	$BB-1$	$BB-2$	$BB-Gap(\%)$	$Time(s)$
10	3	0.3	416	0.032	0	0	-	1.3
	5	0.3	198	0.988	0	0	-	0.7
	7	0.3	261	0.074	0	0	-	0.5
	3	0.5	222	0.894	0	0	-	0.7
	5	0.5	213	0.907	0	0	-	0.6
	7	0.5	256	0.048	0	0	-	0.5
	3	0.7	256	0.978	0	0	-	0.8
	5	0.7	223	0.986	0	0	-	1.3
	7	0.7	262	0.102	0	0	-	1.1
15	3	0.3	971	0.907	0	0	-	15.8
	5	0.3	3918	1.505	6	0	0.927	48.5
	7	0.3	904	0.989	0	0	-	10.4
	3	0.5	3808	1.219	4	0	0.944	47.8
	5	0.5	543	0.994	0	0	-	8.7
	7	0.5	324	0.992	0	0	-	5.6
	3	0.7	5169	1.890	14	0	0.981	64.3
	5	0.7	378	0.992	0	0	-	5.9
	7	0.7	521	0.539	0	0	-	8.6
20	3	0.3	2268	0.999	0	0	-	105.6
	5	0.3	271	0.926	0	0	-	15.6
	7	0.3	877	0.856	0	0	-	53.5
	3	0.5	1091	0.992	0	0	-	51.7
	5	0.5	298	0.932	0	0	-	15.1
	7	0.5	969	0.643	0	0	-	58.9
	3	0.7	1328	0.991	0	0	-	62.2
	5	0.7	439	0.998	0	0	-	22.4
	7	0.7	1203	0.686	0	0	-	68.6
25	3	0.3	10292	2.156	38	2	0.978	1356.4
	5	0.3	498	0.954	0	0	-	73.1
	7	0.3	934	0.666	0	0	-	168.5
	3	0.5	8358	1.952	26	2	0.999	1096.1
	5	0.5	5577	1.078	14	0	0.952	758.4
	7	0.5	1049	0.919	0	0	-	186.7
	3	0.7	7825	1.656	26	0	0.972	1070.7
	5	0.7	687	0.914	0	0	-	103.0
	7	0.7	911	0.821	0	0	-	166.6

Table 7: LR and Branch-and-Bound for *R-MAHLPl* with $\mathbf{q} \in (0, 0.1)$

$\|\mathbf{N}\|$	p	γ	$\#Lagiter.$	$Gap(\%)$	$BB-1$	$BB-2$	$BB-Gap(\%)$	$Time(s)$
10	3	0.3	375	0.963	0	0	-	1.3
	5	0.3	426	0.110	0	0	-	0.9
	7	0.3	253	0.018	0	0	-	1.0
	3	0.5	315	0.001	0	0	-	1.1
	5	0.5	348	0.077	0	0	-	1.3
	7	0.5	249	0.017	0	0	-	0.5
	3	0.7	305	0.000	0	0	-	0.6
	5	0.7	317	0.014	0	0	-	1.2
	7	0.7	235	0.018	0	0	-	1.1
15	3	0.3	1295	0.994	0	0	-	15.6
	5	0.3	437	0.088	0	0	-	5.6
	7	0.3	464	0.316	0	0	-	6.8
	3	0.5	867	0.993	0	0	-	10.7
	5	0.5	389	0.106	0	0	-	6.2
	7	0.5	403	0.127	0	0	-	6.7
	3	0.7	1153	0.997	0	0	-	13.5
	5	0.7	383	0.202	0	0	-	5.3
	7	0.7	375	0.074	0	0	-	6.1
20	3	0.3	1233	0.988	0	0	-	54.2
	5	0.3	415	0.383	0	0	-	19.9
	7	0.3	351	0.387	0	0	-	20.0
	3	0.5	1331	0.996	0	0	-	57.1
	5	0.5	380	0.260	0	0	-	19.1
	7	0.5	415	0.436	0	0	-	23.2
	3	0.7	1338	0.971	0	0	-	58.5
	5	0.7	164	0.990	0	0	-	7.8
	7	0.7	396	0.342	0	0	-	23.3
25	3	0.3	1219	0.997	0	0	-	156.7
	5	0.3	533	0.987	0	0	-	69.0
	7	0.3	473	0.997	0	0	-	64.6
	3	0.5	1060	0.967	0	0	-	138.4
	5	0.5	254	0.987	0	0	-	34.9
	7	0.5	397	0.969	0	0	-	54.6
	3	0.7	960	0.974	0	0	-	124.8
	5	0.7	331	0.909	0	0	-	44.7
	7	0.7	233	0.991	0	0	-	33.6

Table 8: LR and Branch-and-Bound for *R-MAHLPh* with $\mathbf{q} \in (0.2, 0.3)$

$\|\mathbf{N}\|$	p	γ	$\#Lagiter.$	$Gap(\%)$	$BB-1$	$BB-2$	$BB-Gap(\%)$	$Time(s)$
10	3	0.3	305	0.994	0	0	-	1.7
	5	0.3	344	0.965	0	0	-	1.2
	7	0.3	273	0.207	0	0	-	0.5
	3	0.5	337	0.931	0	0	-	1.3
	5	0.5	208	0.991	0	0	-	1.5
	7	0.5	261	0.103	0	0	-	0.6
	3	0.7	296	0.968	0	0	-	1.1
	5	0.7	326	0.172	0	0	-	0.9
	7	0.7	258	0.020	0	0	-	1.0
15	3	0.3	3543	1.401	4	0	0.965	47.5
	5	0.3	3243	1.068	2	0	0.973	41.9
	7	0.3	3797	1.036	8	0	0.999	52.2
	3	0.5	3953	2.087	6	0	0.994	47.1
	5	0.5	418	0.980	0	0	-	5.5
	7	0.5	354	0.984	0	0	-	5.2
	3	0.7	4446	2.010	12	0	0.979	53.8
	5	0.7	1075	0.991	0	0	-	14.1
	7	0.7	503	0.442	0	0	-	8.9
20	3	0.3	1780	0.997	0	0	-	78.4
	5	0.3	950	0.986	0	0	-	43.5
	7	0.3	1054	0.939	0	0	-	50.0
	3	0.5	1061	0.998	0	0	-	45.0
	5	0.5	778	0.820	0	0	-	35.8
	7	0.5	920	0.984	0	0	-	45.1
	3	0.7	1418	0.999	0	0	-	64.1
	5	0.7	867	0.922	0	0	-	30.1
	7	0.7	1795	0.800	0	0	-	85.5
25	3	0.3	5582	2.130	20	0	1.000	740.7
	5	0.3	718	0.990	0	0	-	95.1
	7	0.3	1031	0.988	0	0	-	141.3
	3	0.5	10026	2.595	54	0	0.999	1284.2
	5	0.5	4545	1.200	12	0	0.995	634.7
	7	0.5	1266	0.982	0	0	-	175.8
	3	0.7	7266	2.359	32	0	0.998	981.9
	5	0.7	832	0.990	0	0	-	109.0
	7	0.7	1277	0.996	0	0	-	175.5

including the contribution of backup hubs and alternative routes, as follows.

$$
\begin{aligned}
Psg = & \sum_i \sum_k \sum_m \sum_{j>i} w_{ij}(1 - q_k - q_m^k + q_k q_m^k) X_{ikmj} \\
& + \sum_i \sum_{j>i} \sum_k \sum_{m \neq k} \sum_n w_{ij} q_k (1 - q_n^m)(1 - q_m) X_{ikmj} U_{ijn} \\
& + \sum_i \sum_{j>i} \sum_k \sum_{m \neq k} \sum_n w_{ij} q_m (1 - q_k)(1 - q_n^k) X_{ikmj} V_{ijn} \\
& + \sum_i \sum_{j>i} \sum_k \sum_n w_{ij} q_k (1 - q_n) X_{ikkj} U_{ijn} \\
Mile = & \sum_i \sum_k \sum_m \sum_{j>i} (c_{ik} + c_{km} + c_{mj}) w_{ij} (1 - q_k - q_m^k + q_k q_m^k) X_{ikmj} \\
& + \sum_i \sum_{j>i} \sum_k \sum_{m \neq k} \sum_n (c_{in} + c_{nm} + c_{mj}) w_{ij} q_k (1 - q_n^m)(1 - q_m) X_{ikmj} U_{ijn} \\
& + \sum_i \sum_{j>i} \sum_k \sum_{m \neq k} \sum_n (c_{ik} + c_{kn} + c_{nj}) w_{ij} q_m (1 - q_k)(1 - q_n^k) X_{ikmj} V_{ijn} \\
& + \sum_i \sum_{j>i} \sum_k \sum_n (c_{in} + c_{nj}) w_{ij} q_k (1 - q_n) X_{ikkj} U_{ijn} \\
Cost = & \sum_i \sum_k \sum_m \sum_{j>i} F_{ikmj} w_{ij} (1 - q_k - q_m^k + q_k q_m^k) X_{ikmj} \\
& + \sum_i \sum_{j>i} \sum_k \sum_{m \neq k} \sum_n F_{inmj} w_{ij} q_k (1 - q_n^m)(1 - q_m) X_{ikmj} U_{ijn} \\
& + \sum_i \sum_{j>i} \sum_k \sum_{m \neq k} \sum_n F_{iknj} w_{ij} q_m (1 - q_k)(1 - q_n^k) X_{ikmj} V_{ijn} \\
& + \sum_i \sum_{j>i} \sum_k \sum_n F_{innj} w_{ij} q_k (1 - q_n) X_{ikkj} U_{ijn}
\end{aligned}
$$

We first show that hub locations and spoke allocations of reliable models could be different from those of classical models. Figure 4 demonstrates a case where $|\mathbf{N}| = 15$, $p = 5$, $\gamma = 0.7$, and unavailability $\mathbf{q} \in (0, 0.1)$. Figure 4(a) shows the network configuration obtained by the classical SA hub-and-spoke model and Figure 4(b) shows the network configuration obtained by *R-SAHLP*. Note that initially Cleveland is selected as a hub and it serves Detroit, Baltimore, Boston, Cincinnati and itself. Then, if we consider unavailability, this hub moves to Detroit and Cincinnati leaves this service region and joins in the region served by the hub in Chicago. Under the same hub unavailability, the first network configuration is expected to transport $1,041,280$ passengers and the second is expected to transport $1,112,503$ passengers (by both regular and alternative routes), a 6.84% improvement. In fact, for the second configuration, even we ignore benefits from backup hubs and alternative routes, more passengers, $1,066,010$, can be successfully transported just

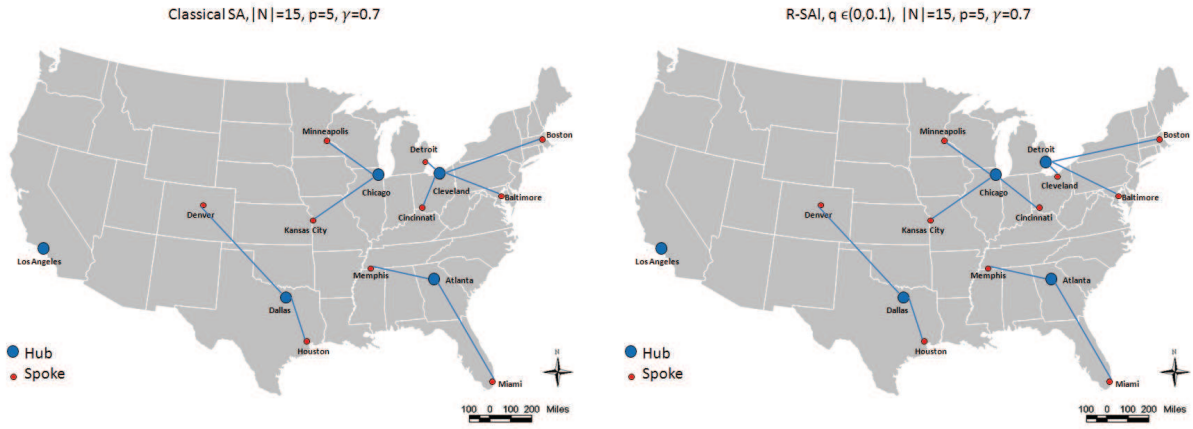

(a) Configuration from Classical Model

(b) Configuration from Reliable Model

Figure 4: System Configurations in Different SA Models

by regular routes, which indicates the importance of including hub unavailability in system design.

We also perform a sensitivity analysis on networks determined by classical and reliable models. We assume that all nodes have the same hub failure probability and investigate the impact of 1% variation in unavailability on the aforementioned performance measures. Both low and high unavailability scenarios are considered with $\mathbf{q} = 0.05$ and $\mathbf{q} = 0.2$ respectively. In Table 9, we report our numerical results for $|\mathbf{N}| = 25$, $p = 5$ and $\gamma = 0.7$ where column *Perf* is to represent the virtual performance measures without variation, column $+1\%$ is to represent the performance when $\mathbf{q}$ is increased by 1%, expressed in terms of percentage of the case without variation.

A clear observation is that all performance measures of reliable hub-and-spoke systems are much less sensitive to variations in availability, which means that they have a higher survivability and are more robust to disruptions. Note also that, reliable models may behave differently from classical models, whose mileage and cost reduction generally are more than the reduction in passengers. This could be explained by the fact that alternative routes through back-up hubs are generally not optimal routes. So, lower hub availability implies that higher percentage of flow is forced to take alternative routes. As a result, compared with the reduction in transported passengers, we probably will have a less reduction in mileage and transportation cost.

Table 9: Sensitivity Analysis in Classical and Reliable Models

		SA				MA			
		Classical		Reliable		Classical		Reliable	
q	$Mea.$	$Perf.$	+1%	$Perf.$	+1%	$Perf.$	+1%	$Perf.$	+1%
0.95	Psg	3917890.000	98.25%	4147880.000	99.37%	3946290.000	98.39%	4152680.000	99.40%
	Mileage($\times 10^6$)	4600.250	98.03%	4929.560	99.33%	3820.210	98.20%	4289.760	99.56%
	Cost($\times 10^6$)	3717.450	98.06%	4026.500	99.57%	3135.880	98.26%	3669.440	99.77%
0.8	Psg	2949110.000	97.97%	3845050.000	99.21%	3044770.000	98.15%	3902540.000	99.32%
	Mileage($\times 10^6$)	3333.010	97.68%	4663.800	99.17%	2851.990	97.91%	4286.320	99.39%
	Cost($\times 10^6$)	2706.980	97.72%	4062.370	99.34%	2366.710	97.99%	3863.430	99.54%

Table 10: Performance with $\mathbf{q} \in (0, 0.1)$ in SA Hub-and-spoke System

		Classical *SAHLP*			*R-SAHLP*					
$\|\mathbf{N}\|$	p	*Psg*	*Mileage* ($\times 10^6$)	*Cost* ($\times 10^6$)	*Psg*	*Psg* %	*Mileage* ($\times 10^6$)	*Mileage* %	*Cost* ($\times 10^6$)	*Cost* %
10	3	483672.000	384.298	329.722	487006.680	100.69%	387.973	100.96%	333.310	101.09%
	5	474514.000	330.681	266.526	476577.480	100.43%	332.613	100.58%	268.351	100.68%
	7	444315.000	295.299	217.480	469115.640	105.58%	314.980	106.66%	234.643	107.89%
15	3	1056350.000	1280.550	1116.990	1128935.600	106.87%	1407.444	109.91%	1233.740	110.45%
	5	1041280.000	1170.340	946.486	1112503.400	106.84%	1247.990	106.63%	1021.888	107.97%
	7	1028370.000	1083.260	832.522	1104016.000	107.36%	1164.357	107.49%	908.172	109.09%
20	3	2664270.000	3200.500	2721.910	2849878.500	106.97%	3401.709	106.29%	2989.854	109.84%
	5	2645620.000	2920.360	2286.020	2790963.500	105.49%	2985.364	102.23%	2500.755	109.39%
	7	2672940.000	2691.170	2047.140	2762045.700	103.33%	2745.864	102.03%	2187.902	106.88%
25	3	3814480.000	4834.970	4139.160	4140867.000	108.56%	5334.822	110.34%	4622.952	111.69%
	5	3798480.000	4451.710	3596.760	4098919.000	107.91%	4867.152	109.33%	3988.245	110.88%
	7	3846820.000	4307.930	3354.980	4096211.000	106.48%	4567.190	106.02%	3645.522	108.66%

Table 11: Performance with $\mathbf{q} \in (0.2, 0.3)$ in SA Hub-and-spoke System

		Classical *SAHLP*			*R-SAHLP*					
$\|\mathbf{N}\|$	p	*Psg*	*Mileage* ($\times 10^6$)	*Cost* ($\times 10^6$)	*Psg*	*Psg* %	*Mileage* ($\times 10^6$)	*Mileage* %	*Cost* ($\times 10^6$)	*Cost* %
10	3	334994.000	258.798	224.242	430891.300	128.63%	353.698	136.67%	320.904	143.11%
	5	319420.000	217.127	176.775	400287.200	125.32%	301.375	138.80%	257.918	145.90%
	7	284662.000	185.286	136.982	340028.700	119.45%	226.088	122.02%	177.683	129.71%
15	3	753076.000	875.355	774.143	1039288.000	138.01%	1333.571	152.35%	1235.060	159.54%
	5	683101.000	742.555	603.914	883401.000	129.32%	963.151	129.71%	851.201	140.95%
	7	666205.000	681.373	526.694	913019.000	137.05%	1007.556	147.87%	884.054	167.85%
20	3	1870270.000	2142.950	1844.930	2588927.000	138.43%	3117.535	145.48%	2868.176	155.46%
	5	1786700.000	1870.090	1474.520	2476424.000	138.60%	2700.856	144.42%	2359.015	159.99%
	7	1761160.000	1707.610	1304.690	2437349.000	138.39%	2564.805	150.20%	2193.559	168.13%
25	3	2670530.000	3208.470	2779.440	3835310.000	143.62%	4968.590	154.86%	4635.600	166.78%
	5	2557360.000	2836.750	2308.480	3738470.000	146.18%	4537.720	159.96%	4005.290	173.50%
	7	2545000.000	2721.530	2130.800	3645365.000	143.24%	4201.780	154.39%	3560.430	167.09%

Table 12: Performance with $\mathbf{q} \in (0, 0.1)$ in MA Hub-and-spoke System

		Classical *MAHLP*			*R-MAHLP*					
$\|\mathbf{N}\|$	p	*Psg*	*Mileage* ($\times 10^6$)	*Cost* ($\times 10^6$)	*Psg*	*Psg* %	*Mileage* ($\times 10^6$)	*Mileage* %	*Cost* ($\times 10^6$)	*Cost* %
10	3	484020.000	320.684	293.459	487014.550	100.62%	324.539	101.20%	297.163	101.26%
	5	475636.000	304.996	249.254	477780.760	100.45%	307.437	100.80%	251.435	100.88%
	7	461799.000	286.453	217.037	469103.130	101.58%	294.021	102.64%	225.012	103.67%
15	3	1072890.000	115.854	1048.610	1129684.400	105.29%	1234.498	106.56%	1141.760	108.88%
	5	1052460.000	1023.310	865.660	1112734.500	105.73%	1106.319	108.11%	945.105	109.18%
	7	1054940.000	1006.550	795.844	1110345.200	105.25%	1079.437	107.24%	865.891	108.80%
20	3	2709420.000	2712.100	2470.900	2786861.000	102.86%	2804.623	103.41%	2624.291	106.21%
	5	2692590.000	2473.400	2058.820	2760083.400	102.51%	2592.616	104.82%	2195.410	106.63%
	7	2637760.000	2367.220	1877.960	2752731.300	104.36%	2514.436	106.22%	2033.166	108.26%
25	3	3919110.000	4228.020	3845.110	4215926.000	107.57%	4672.984	110.52%	4261.154	110.82%
	5	3866730.000	3866.610	3291.980	4109341.000	106.27%	4251.163	109.94%	3649.801	110.87%
	7	3885230.000	3760.510	3088.380	4201039.000	108.13%	4226.028	112.38%	3568.934	115.56%

Table 13: Performance with $\mathbf{q} \in (0.2, 0.3)$ in MA Hub-and-spoke System

		Classical *MAHLP*			*R-MAHLP*					
$\|\mathbf{N}\|$	p	*Psg*	*Mileage* ($\times 10^6$)	*Cost* ($\times 10^6$)	*Psg*	*Psg* %	*Mileage* ($\times 10^6$)	*Mileage* %	*Cost* ($\times 10^6$)	*Cost* %
10	3	358315.000	231.396	214.183	448768.200	120.48%	314.667	135.99%	305.418	142.60%
	5	337120.000	207.503	172.488	385303.900	110.10%	244.045	117.61%	219.323	127.15%
	7	310787.000	185.376	142.067	370951.600	115.15%	228.201	123.10%	203.261	143.07%
15	3	795025.000	832.446	764.234	1101870.000	130.69%	1194.725	143.52%	1165.794	152.54%
	5	747401.000	696.297	599.035	1041114.000	131.04%	1022.345	146.83%	955.909	159.57%
	7	725324.000	660.828	530.297	1010170.000	129.77%	948.119	143.47%	867.159	163.52%
20	3	2037390.000	1982.280	1832.010	2794006.000	128.88%	2888.841	145.73%	2752.820	150.26%
	5	1946850.000	1696.770	1438.040	2742396.000	128.51%	2472.282	145.71%	2261.765	157.28%
	7	1819300.000	1555.310	1250.410	2711165.000	133.33%	2333.067	150.01%	2094.218	167.48%
25	3	2929680.000	3055.560	2818.890	4252980.000	131.65%	4704.340	153.96%	4455.030	158.04%
	5	2790990.000	2641.240	2286.620	4103220.000	134.94%	4090.460	154.87%	3746.180	163.83%
	7	2714620.000	2509.950	2093.060	4077430.000	135.71%	3854.350	153.56%	3399.880	162.44%

Finally, we present a systematic performance comparison between classical and reliable hub-and-spoke models with discount factor γ set to 0.7. All the results are listed in Table 10-13 with the performance measures of reliable models expressed in terms of percentage of those in classical models. We observe that: (i) reliable models can handle disruptions better and transport more passengers, especially for the high unavailability situation. Such an improvement is more significant for SA networks, which can be explained by the fact that regular routes in SA structure are less flexible and less robust while alternative routes are selected according to MA structure; (ii) among all instances, the improvement in transported passengers is larger if problem scale is larger. This could be explained by the fact that non-transportable flows in alternative routes, i.e. those from disrupted hubs, have a smaller portion in total flows for larger $|\mathbf{N}|$; (iii) the cost and milage increase more than the passengers. This could be explained using the same explanation to our observation in sensitivity analysis: the alternative routes are longer and have less economic advantages. In fact, the cost increases more than the milage, which indicates that more or longer spoke-hub arcs are used in alternative routes than in regular routes.

Furthermore, in Figure 5, we interestingly observe a strong linear correlation between percentage values of the additional transported passengers and the additional transportation cost for reliable hub-and-spoke models. Note that transporting 1% more passengers leads to 1.8658% cost increases in *R-MAHLP* while it leads to 1.6125% cost increases in *R-SAHLP*. Such a result indicates that the reliable network design has better relative economic advantages in SA model than in MA model. This could be explained by two facts that MA structure is used in designing alternative routes for both reliable SA and MA networks and regular routes in SA network generate more cost than those in MA network. We point out that linear regression results in both reliable SA and MA models have very high R^2 values. Thus, the obtained regression functions can be considered as reliable prediction tools to estimate the extra cost of transporting more passengers. Although we believe that those results and their implications will be useful for airlines to solve the pricing problem in disruption management, it is beyond the scope of this paper and will be investigated in future.

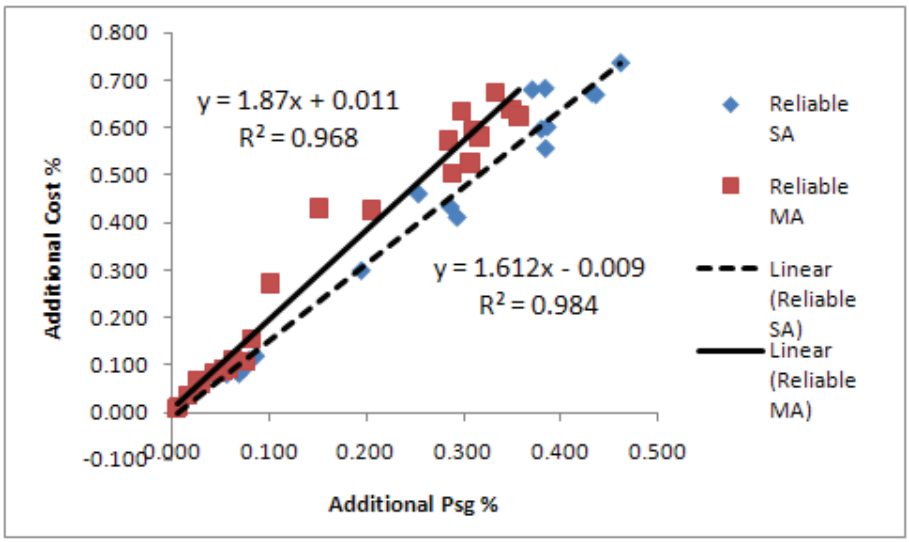

Figure 5: Regression between Additional Cost and Passengers

6 Conclusions

In this paper, we construct reliable single allocation and multiple allocation hub-and-spoke models that generalize their classical counterparts. Given the fact that the performance of a hub-and-spoke network is heavily dependant on the availability of a small number of hubs, our models seek to build hub-and-spoke systems with backup hubs and alternative routes to better hedge against various disruptive situations in practice. Due to the complexity of the reliable models, we develop a set of Lagrangian relaxation/Branch-and-Bound algorithms that are easy to implement and can compute optimal solutions efficiently. Our computational study shows that those algorithms drastically outperform the state-of-the-art commercial mixed integer program solver, CPLEX, with two types of linearized models. Our numerical study indicates that hub-and-spoke network design is sensitive to the nodes' (airports') availability and the reliable design paradigm generates networks with significantly higher survivability in disruptive situations. In fact, those models and algorithms are flexible to deal with different situations, such as just allowing a subset of flows to be rerouted, with little modification. Therefore, system designers can use them to derive the optimal system design with a desired trade-off among various performance measures.

To the best of our knowledge, our work is the first analytical study on reliable hub-and-spoke network design problem. It theoretically extends the existing literature on reliable

network design and also has a clear practical impact on transportation and telecommunications systems. Also, we provide efficient solution methods to support the study and application of those models on real size instances. One possible research direction is using those models and the solution algorithms to investigate the pricing problem if backup hubs and alternative routes are employed to deal with disrupted air transportation. Another direction is to jointly consider queuing effect, i.e. hub congestion cost, and hub availability in hub-and-spoke network design, which will demand more efficient computing tools to derive the optimal solution.

References

[1] Airportwatch. April, 27, 2010. Volcanic ash crisis cost airlines 2.2 billion. *Airportwatch* URL `http://airportwatch.org.uk/news/detail.php?art_id=4021`.

[2] Alumur, S., B. Y. Kara. 2008. Network hub location problems: The state of the art. *European Journal of Operational Research* **190**(1) 1–21.

[3] Ball, M., C. Barnhart, G. Nemhauser, A. Odoni. 2006. Air transportation: irregular operations and control. *Handbooks of Operations Research and Management*. North-Holland.

[4] Campell, J. F. 1994. Integer programming formulations of discrete hub location problems. *European Journal of Operational Research* **72**(2) 387–405.

[5] Cánovas, L., S. García, A. Marín. 2007. Solving the uncapacitated multiple allocation hub location problem by means of a dual-ascent technique. *European Journal of Operational Research* **179**(3) 900–1007.

[6] Chaovalitwongse, W., P. M. Pardalos, O. A. Prokopyev. 2004. A new linearization technique for multi-quadratic 0-1 programming problems. *Operations Research Letters* **32**(6) 517–522.

[7] Chen, J. 2007. A hybrid heuristic for the uncapacitated single allocation hub location problem. *Omega* **35**(2) 211–220.

[8] Contreras, I., J. Cordeau, G. Laporte. 2011. The dynamic uncapacitated hub location problem. *Transportation Science* **45**(1) 18–32.

[9] Cui, T., Y. Ouyang, Z. M. Shen. 2010. Reliable facility location design under the risk of disruptions. *Operations Research* **58**(4) 998–1011.

[10] Cunha, C. B., M. R. Silva. 2007. A genetic algorithm for the problem of configuring a hub-and-spoke network for a LTL trucking company in brazil. *European Journal of Operational Research* **179**(3) 747–758.

[11] de Camargo, R. S., G. Miranda, Jr., R. P. Ferreira, H. P. Luna. 2009. Multiple allocation hub-and-spoke network design under hub congestion. *Computers & Operations Research* **36**(12) 3097–3106.

[12] de Camargo, R. S., G. Miranda, Jr., H. P. Luna. 2009. Benders decomposition for hub location problems with economies of scale. *Transportation Science* **43**(1) 86–97.

[13] Elhedhli, S., F. X. Hu. 2005. Hub-and-spoke network design with congestion. *Computers & Operations Research* **32**(6) 1615–1632.

[14] Elhedhli, S., H. Wu. 2010. A lagrangean heuristic for hub-and-spoke system design with capacity selection and congestion. *Informs Journal on Computing* **22**(2) 282–296.

[15] Ernst, A. T., M. Krishnamoorthy. 1996. Efficient algorithms for the uncapacitated single allocation p-hub median problem. *Location Science* **4**(3) 139–154.

[16] Ernst, A. T., M. Krishnamoorthy. 1998. Exact and heuristic algorithms for the uncapacitated multiple allocation p-hub median problem. *European Journal of Operational Research* **104**(1) 100–112.

[17] Ernst, A. T., M. Krishnamoorthy. 1998. An exact solution approach based on shortest-paths for p-hub median problems. *Informs Journal on Computing* **10**(2) 149–162.

[18] Fisher, M. L. 2004. The Lagrangian relaxation method for solving integer programming problems. *Management science* **50** 1861–1871.

[19] Grove, G. P., M. E. O'Kelly. 1986. Hub networks and simulated schedule delay. *Papers of The Regional Science Association* **59**(1) 103–119.

[20] Hamacher, H. W., M. Labbé, S. Nickle, T. Sonneborn. 2000. Polyhedral properties of the uncapacitated multiple allocation hub location problem. Tech. rep., Institut für Techno und Wirtschaftsmathematik (ITWM), Kaiserslautern, Germany.

[21] Hamacher, H. W., M. Labbé, S. Nickle, T. Sonneborn. 2004. Adapting polyhedral properties from facitily to hub location problems. *Discrete Applied Mathematics* **145**(1) 104–116.

[22] He, X., A. Chen, W. A. Chaovalitwongse, H. X. Liu. 2010. An improved linearization technique for a class of quadratic 0-1 programming problems. *Optimization Letters, published online* 1–11.

[23] Janic, M. 2005. Modeling the large scale disruption of an airline network. *Journal of Transportation Engineering* **131**(4) 249–260.

[24] Kim, H., M. E. O'Kelly. 2009. Reliable p-hub location problems in telecommunication networks. *Geographical Analysis* **41**(3) 283–306.

[25] Li, Q., B. Zeng, A. Savachkin. 2011. Decision support models for design of reliable distribution networks. *under review* .

[26] Li, X., Y. Ouyang. 2010. A continuum approximation approach to reliable facility location design under correlated probabilistic disruptions. *Transportation Research Part B* **44**(4) 535–548.

[27] Li, X., Y. Ouyang. 2011. Reliable sensor deployment for network traffic surveillance. *Transportation Research Part B: Methodological* **45** 218–231.

[28] Lim, M., M. S. Daskin, A. Bassamboo, S. Chopra. 2009. A facility reliability problem: Formulation, properties, and algorithm. *Naval Research Logistics* **57**(1) 58–70.

[29] Nemhauser, G. L., L. A. Wolsey. 1988. *Integer and Combinatorial Optimization*. Wiley.

[30] O'Kelly, M. E. 1986. Activity levels at hub facilities in interacting networks. *Geographical Analysis* **18**(4) 343–356.

[31] O'Kelly, M. E. 1986. The location of interacting hub facilities. *Transportation Science* **20**(2) 92–105.

[32] O'Kelly, M. E. 1987. A quadratic integer program for the location of interacting hub facilities. *European Journal of Operational Research* **32**(3) 393–404.

[33] O'Kelly, M. E. 1992. Hub facility location with fixed costs. *Papers in Regional Science* **71**(3) 293–306.

[34] O'Kelly, M. E., H. Kim, C. Kim. 2006. Internet reliability with realistic peering. *Environment and Planning Part B* **33**(3) 325–343.

[35] Pirkul, H., D. A. Schilling. 1998. An efficient procedure for designing single allocation hub and spoke systems. *Management Science* **44**(12) S235–S242.

[36] Sherali, H. D., J. C. Smith. 2007. An improved linearization strategy for zero-one quadratic programming problems. *Optimization Letters* **1**(1) 33–47.

[37] Skorin-Kapov, D., J. Skorin-Kapov, M. E. O'Kelly. 1996. Tight linear programming relaxations of uncapacitated p-hub median problems. *European Journal of Operational Research* **94**(3) 582–593.

[38] Snyder, L. V., M. S. Daskin. 2005. Reliability models for facility location: The expected failure cost case. *Transportation Science* **39**(3) 400–416.

[39] Zeng, B., Y. An, Y. Zhang, H. Kim. 2010. A reliable hub-spoke model in transportation systems. *The 4th International Symposium on Transportation Network Reliability (INSTR) Conference Proceedings*.